Published OnlineFirst April 9, 2021; DOI: 10.1158/2159-8290.CD-20-1661

RESEARCH ARTICLE

IFNγ Is Critical for CAR T Cell–Mediated Myeloid Activation and Induction of Endogenous Immunity

Darya Alizadeh[1], Robyn A. Wong[1], Sharareh Gholamin[2], Madeleine Maker[1], Maryam Aftabizadeh[1], Xin Yang[1], Joseph R. Pecoraro[1], John D. Jeppson[1], Dongrui Wang[1], Brenda Aguilar[1], Renate Starr[1], Claire B. Larmonier[3], Nicolas Larmonier[4], Min-Hsuan Chen[5], Xiwei Wu[5], Antoni Ribas[6], Behnam Badie[7], Stephen J. Forman[1], and Christine E. Brown[1]

Published OnlineFirst April 9, 2021; DOI: 10.1158/2159-8290.CD-20-1661

ABSTRACT Chimeric antigen receptor (CAR) T cells mediate potent antigen-specific antitumor activity; however, their indirect effects on the endogenous immune system are not well characterized. Remarkably, we demonstrate that CAR T-cell treatment of mouse syngeneic glioblastoma (GBM) activates intratumoral myeloid cells and induces endogenous T-cell memory responses coupled with feed-forward propagation of CAR T-cell responses. IFNγ production by CAR T cells and IFNγ responsiveness of host immune cells are critical for tumor immune landscape remodeling to promote a more activated and less suppressive tumor microenvironment. The clinical relevance of these observations is supported by studies showing that human IL13Rα2–CAR T cells activate patient-derived endogenous T cells and monocytes/macrophages through IFNγ signaling and induce the generation of tumor-specific T-cell responses in a responding patient with GBM. These studies establish that CAR T-cell therapy has the potential to shape the tumor microenvironment, creating a context permissible for eliciting endogenous antitumor immunity.

SIGNIFICANCE: Our findings highlight the critical role of IFNγ signaling for a productive CAR T-cell therapy in GBM. We establish that CAR T cells can activate resident myeloid populations and promote endogenous T-cell immunity, emphasizing the importance of host innate and adaptive immunity for CAR T-cell therapy of solid tumors.

INTRODUCTION

Glioblastoma (GBM) is among the deadliest cancers, with very limited therapeutic options (1, 2). Despite aggressive standard-of-care therapies, tumor recurrence is almost inevitable and uniformly lethal, with most patients not surviving beyond two years from diagnosis. Although advances in immunotherapy have resulted in significant therapeutic improvements for many cancers, outcomes for patients with GBM have been disappointing (3). The complex myeloid-rich tumor microenvironment (TME) and heterogeneous nature of GBM remain barriers to the therapeutic success of immunotherapeutic approaches, including checkpoint blockade, vaccine therapy, and chimeric antigen receptor (CAR) T-cell therapy. A better understanding of the interplay between immunotherapy and the TME is required to develop more effective therapies for GBM and other solid tumors.

[1]T Cell Therapeutics Research Labs, Cellular Immunotherapy Center, Department of Hematology and Hematopoietic Cell Transplantation, City of Hope, Duarte, California. [2]Department of Biology and Bioengineering, California Institute of Technology, Pasadena, California. [3]Department of Biopathology, Molecular Pathology Unit, Bergonié Institute, Comprehensive Cancer Center, Bordeaux, France. [4]CNRS UMR 5164, ImmunoConcEpT, University of Bordeaux, Bordeaux, France. [5]Core of Integrative Genomics, City of Hope Comprehensive Cancer Center, Duarte, California. [6]Department of Medicine, Jonsson Comprehensive Cancer Center at University of California, Los Angeles, California. [7]Division of Neurosurgery, Department of Surgery, City of Hope, Duarte, California.

Note: Supplementary data for this article are available at Cancer Discovery Online (http://cancerdiscovery.aacrjournals.org/).

Corresponding Authors: Christine E. Brown, Department of Hematology/HCT, TCTRL, City of Hope, Duarte, CA 91010. Phone: 626-256-4673, ext. 83977; Fax: 626-301-8978; E-mail: cbrown@coh.org; and Darya Alizadeh, Department of Hematology/HCT, TCTRL, City of Hope, Duarte, CA 91010. E-mail: dalizadeh@coh.org

Cancer Discov 2021;11:2248–65

doi: 10.1158/2159-8290.CD-20-1661

CAR T-cell therapy is emerging as a promising strategy to treat cancer and may offer new therapeutic options for individuals diagnosed with GBM and other refractory brain tumors (4). Current efforts are focusing on expanding CAR T-cell targets to address tumor heterogeneity (5–7), armored CAR T cells introducing cytokines to improve CAR T-cell persistence and potency (8–10), and optimizing route of delivery to improve trafficking (11). These preclinical studies have primarily utilized immunocompromised xenograft models to optimize antigen-dependent effector activity. However, to adequately address parameters that are critical for the therapeutic success of CAR T-cell therapy, preclinical models that take into consideration the host immune system are required. Recent studies in immunocompetent models of GBM establish a dynamic interplay between the endogenous immune system and CAR T-cell responses, with phenotypic changes in the immune subsets observed posttherapy (12, 13). Nevertheless, detailed phenotypic analysis of these changes, as well as a mechanistic understanding of whether alterations in the TME may be a consequence of antigen-dependent tumor lysis or indirectly through CAR T cell–mediated cytokine production, have not been well elucidated.

Proinflammatory cytokines secreted by CAR T cells, such as IFNγ, may play an important role in activation and programming of the immune infiltrates in GBM TME. IFNγ can activate macrophage (14) and microglia (15), recruit and activate cytotoxic T cells, polarize $CD4^+$ T cells into Th1 effector cells, and impair tumor-promoting regulatory T cell (Treg) development and function (16–18). IFNs can additionally act as a key signal 3 to facilitate the activation and priming of tumor-reactive T cells (19). Therefore, investigating the potential indirect effects of CAR T-cell therapy on innate immune activation and adaptive immunity is critical for further optimization of this therapy for solid tumors.

Although CAR T-cell therapy in GBM and other solid tumors has not elicited the remarkable responses observed in hematologic malignancies, clinical studies have demonstrated

Published OnlineFirst April 9, 2021; DOI: 10.1158/2159-8290.CD-20-1661

early evidence of safety and bioactivity in selected patients (20–24). Our lead CAR program for GBM targets IL13Rα2, a tumor-associated antigen that is overexpressed by the majority of GBM (25). We previously optimized an IL13 (E12Y)-ligand 4-1BB/CD137–based CAR for clinical translation (6) and have initiated a phase I trial to evaluate the safety and feasibility of locoregionally delivered IL13Rα2-CAR T cells for recurrent GBM. While this trial is ongoing, one patient of particular interest, who presented with recurrent multifocal GBM, remarkably achieved a complete response (CR) following locoregional delivery of IL13Rα2-CAR T cells, despite heterogeneous IL13Rα2 tumor expression. This case study demonstrates that CAR T-cell therapy has the potential to elicit profound antitumor activity against one of the most difficult-to-treat solid tumors. Lessons learned from this clinical experience as well as other early clinical findings for CAR T cells in GBM suggest that in addition to targeting antigen-positive cells, CAR T cells may also alter the TME with local changes in inflammatory cytokines, alterations in tumor immune infiltrates, and clonal T-cell populations (20–22). However, very little is understood regarding the therapeutic dependencies between CAR T-cell therapy and the endogenous immune system.

Herein, we evaluated changes in the TME post–CAR T-cell therapy in both murine immunocompetent mouse models and patient-derived immune populations. Focusing on our clinically validated IL13Rα2-CAR T-cell platform, we show that CAR T cells not only target antigen-positive tumors, but also promote the activation of host immune cells in the TME through a mechanism involving IFNγ signaling. Our findings highlight that CAR T-cell therapy changes GBM immune landscape and induces activation of host immune cells, which in turn can enhance CAR T-cell therapy. Defining the immunologic changes potentiated by CAR T-cell therapy, along with specific immunologic signatures required for effective antitumor responses, is critical for the successful advancement of CAR T-cell therapy for solid tumors.

RESULTS

CAR T Cells Induce Endogenous Antitumor Immune Responses in GBM Patient Unique Responder

Motivated by the unique responder in our IL13Rα2–CAR clinical trial, in which locoregionally delivered CAR T cells mediated a CR in a setting of progressive multifocal GBM, we set out to investigate whether CAR T cells may have stimulated endogenous immunity that could have cooperated with CAR T-cell therapy to elicit this profound therapeutic response (20). To determine whether this clinical response involved the induction of host immunity, T cells were isolated from the patient's blood before CAR T-cell treatment (pre-CAR T) and during the response to CAR T-cell therapy (post-CAR T; Fig. 1A). Isolated $CD3^+$ T cells, confirmed to be CAR-negative (Supplementary Fig. S1), were stimulated and expanded in the presence of the patient's irradiated autologous tumor cell line. Endogenous CAR-negative T cells isolated during response (post-CAR T) displayed enhanced tumor reactivity as indicated by increased intracellular IFNγ (3.9-fold increase) and greater tumor-dependent proliferation as compared with T cells isolated prior to the initiation of CAR T-cell therapy (pre-CAR T; Fig. 1B and C). Importantly, subsequent coculture assays with the autologous patient GBM tumor line or an irrelevant tumor line established that T cells isolated during response to CAR T-cell therapy exhibited enhanced tumor-specific killing compared with pretreatment T cells (Fig. 1D). Tumor-specific proliferation and killing by endogenous T cells isolated from the blood during therapeutic response was independent of IL13Rα2 expression, as the *ex vivo*–expanded autologous GBM line did not express the IL13Rα2 antigen (Fig. 1E). The same observation was not detected in a patient with GBM who responded poorly to CAR T-cell therapy (Supplementary Fig. S2A–S2D). These findings support the premise that the induction of endogenous immunity is important for productive CAR T-cell therapy and is highly patient dependent, likely influenced by unique aspects of each tumor and the TME. Furthermore, these observations provided the rationale to mechanistically investigate the potential of CAR T cells to promote the generation of tumor-specific T-cell responses as well as evaluate the importance of host immune cells in a successful CAR T-cell therapy.

Murine IL13Rα2–CAR T Cells Mediate Potent Antitumor Activity in Immunocompetent Models of GBM

To gain a deeper understanding of the interplay between CAR T cells, the host immune responses, and the GBM microenvironment, as well as interrogate the potential mechanisms involved (6, 20), we established immunocompetent mouse models of our clinical IL13Rα2-CAR T-cell platform. A mouse counterpart to our human IL13Rα2-targeted CAR was constructed (6), and composed of the IL13 tumor-targeting domain, murine CD8 hinge (mCD8h), murine CD8 transmembrane domain (mCD8tm), murine 4-1BB costimulatory domain (m4–1BB), and murine CD3 zeta (mCD3ζ). A T2A skip sequence separates the CAR from a truncated murine CD19 (mCD19t) used for cell tracking (Supplementary Fig. S3A). The engineering process resulted in a 70% to 85% transduction efficiency as assessed by the frequency of $CD19t^+$ cells (Supplementary Fig. S3B). Phenotypic analyses indicated that, similar to human CAR T cells (6), the murine IL13Rα2-targeted CAR T cells (mIL13BBζ CAR T cells) contained comparable numbers of $CD4^+$ and $CD8^+$ T-cell subsets with mixed early memory ($CD62L^+$) and effector ($CD62L^-$) T-cell populations on day 4 of *ex vivo* expansion (Supplementary Fig. S3C and S3D). We designed a therapeutic setting based on K-Luc and GL261-Luc, two syngeneic, immunocompetent murine glioma models. K-Luc, a firefly luciferase (ffluc)–engineered subline of KR158 (26), was used as it recapitulates the highly invasive features of GBM (Supplementary Fig. S3E). This tumor line is derived from a spontaneous glioma arising from *Nf1, Trp53* mutant mice, and is poorly immunogenic as indicated by its unresponsiveness to anti–PD-1 checkpoint therapy (27). As a second model, we also used GL261 engineered to express ffLuc (GL261-luc), a noninvasive "bulky" glioma (Supplementary Fig. S3F), which was generated by chemical induction, contains high numbers of mutations, and, in contrast to K-Luc, is responsive to anti–PD-1 immunotherapy (28, 29). Both tumor lines were engineered to express murine IL13Rα2 (mIL13Rα2; Supplementary Fig. S3E and S3F). mIL13BBζ CAR T cells specifically killed

Published OnlineFirst April 9, 2021; DOI: 10.1158/2159-8290.CD-20-1661

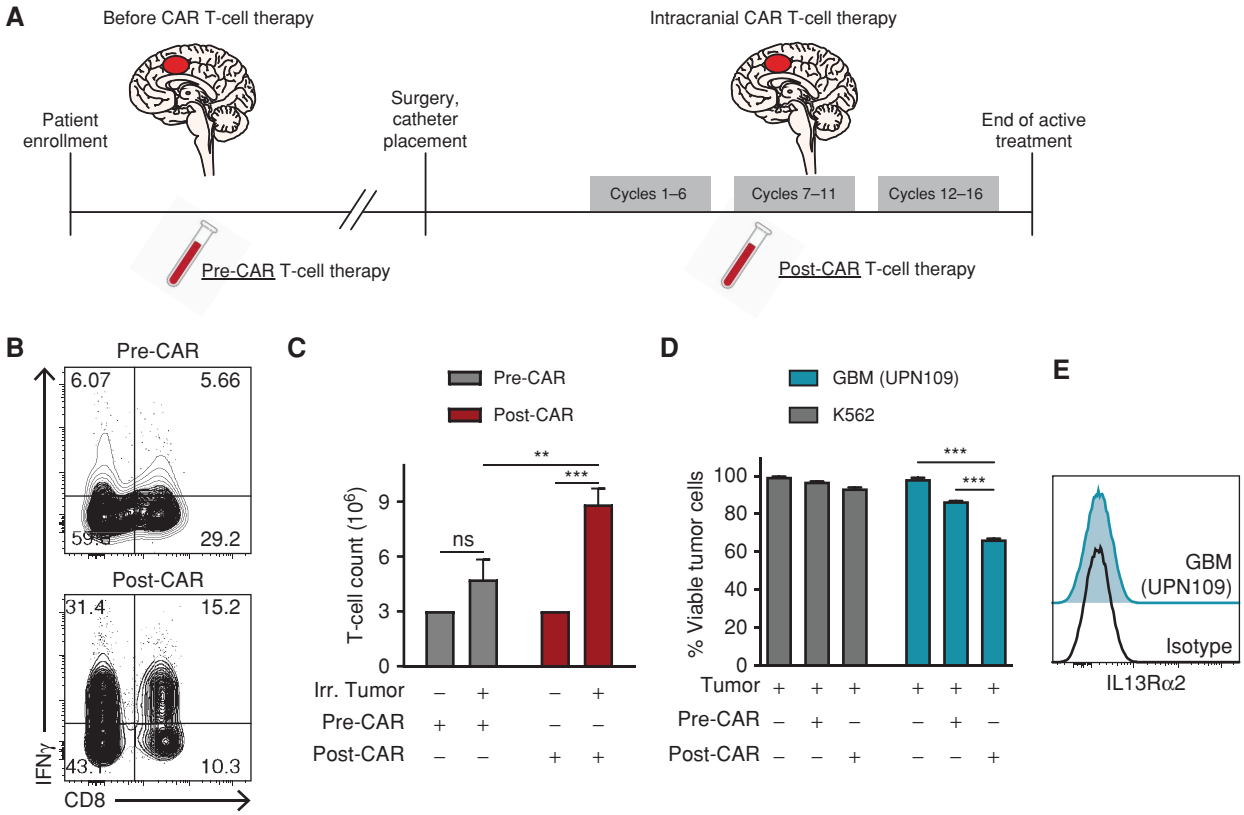

Figure 1. CAR T-cell therapy stimulates endogenous tumor-specific T-cell responses. **A,** Treatment schema of a unique responder to IL13Rα2-CAR T-cell therapy. T cells (CD3$^+$) were isolated from peripheral blood prior to the initiation of therapy (pre-CAR T) and during therapeutic response (post-CAR). **B,** Representative flow cytometry showing intracellular IFNγ levels in patient T cells obtained before therapy (pre-CAR) and during response (post-CAR). T cells were cocultured with irradiated autologous tumor (UPN109) followed by a 4-hour stimulation. **C,** T-cell count after 14-day coculture with autologous irradiated (Irr.) patient tumor cell line. **D,** *In vitro* killing by patient T cells against autologous (UPN109) or nonspecific tumor line (K562). **E,** Representative flow cytometry demonstrates the IL13Rα2 expression of the patient autologous (UPN109) tumor line. Data are presented as means ± SEM (**C** and **D**) and were analyzed by two-tailed, unpaired Student *t* test. *, $P < 0.05$; **, $P < 0.01$; ***, $P < 0.001$; ****, $P < 0.0001$ for indicated comparison.

mIL13Rα2-engineered K-Luc and GL261-Luc cells, which was associated with production of inflammatory cytokines IFNγ and TNFα (Supplementary Fig. S3E and S3F), and were not responsive to IL13Rα2-negative parental tumor lines *in vitro* (Supplementary Fig. S3G).

We next evaluated CAR T-cell antitumor activity against orthotopically engrafted glioma tumors in C57BL/6 immunocompetent mice. In IL13Rα2$^+$ K-Luc tumor model, single intratumoral administration of mIL13BBζ CAR T cells seven days after tumor injection mediated potent *in vivo* antitumor activity and conferred a significant survival benefit (Fig. 2A–D). Mock T-cell or PBS-injected (untreated) tumor-bearing mice did not exhibit reduced tumor progression (Supplementary Fig. S4A) and local treatment of CAR or mock T cells did not result in toxicity-associated weight loss (Supplementary Fig. S4B). To evaluate the impact of an intact immune system on CAR T cell–mediated antitumor responses, we compared anti–K-Luc activity in C57BL/6 mice to tumors engrafted in immunocompromised NOD/SCID IL2Rγnull (NSG) models, which lack adaptive immune subsets. In a smaller tumor model (4 days old), with a less-developed TME, antitumor activity in C57BL/6 and NSG mice was equivalent, indicating CAR T-cell functionality is comparable in both mouse strains and independent of an intact immune system (Supplementary Fig. S5A–S5C). However, surprisingly, the *in vivo* response to CAR T-cell therapy was superior in immunocompetent C57BL/6 as compared with immunodeficient NSG mice ($P < 0.001$) when the TME exhibited an established immune microenvironment (7-day engrafted tumor; Supplementary Fig. S5D and S5E). This observation raised the possibility that tumor-infiltrating immune cells may enhance the antitumor effects of CAR T-cell therapy in GBM, and we sought to further investigate this observation in greater detail.

CAR T-cell Therapy Can Promote Immunologic Memory and the Generation of Tumor-Specific T Cells

To evaluate whether CAR T cells have the potential to induce endogenous antitumor immunity, cured mice following CAR T-cell treatment were challenged with IL13Rα2-negative parental tumors. Indeed, in a more established TME (7-day engraftment before CAR T-cell therapy), cured mice in the immunocompetent C57BL/6 model successfully rejected tumor rechallenge with IL13Rα2-negative K-Luc (Fig. 2E and F) and GL261-Luc (Supplementary Fig. S6A and S6B) parental tumor cells, demonstrating that CAR T cells can promote

Published OnlineFirst April 9, 2021; DOI: 10.1158/2159-8290.CD-20-1661

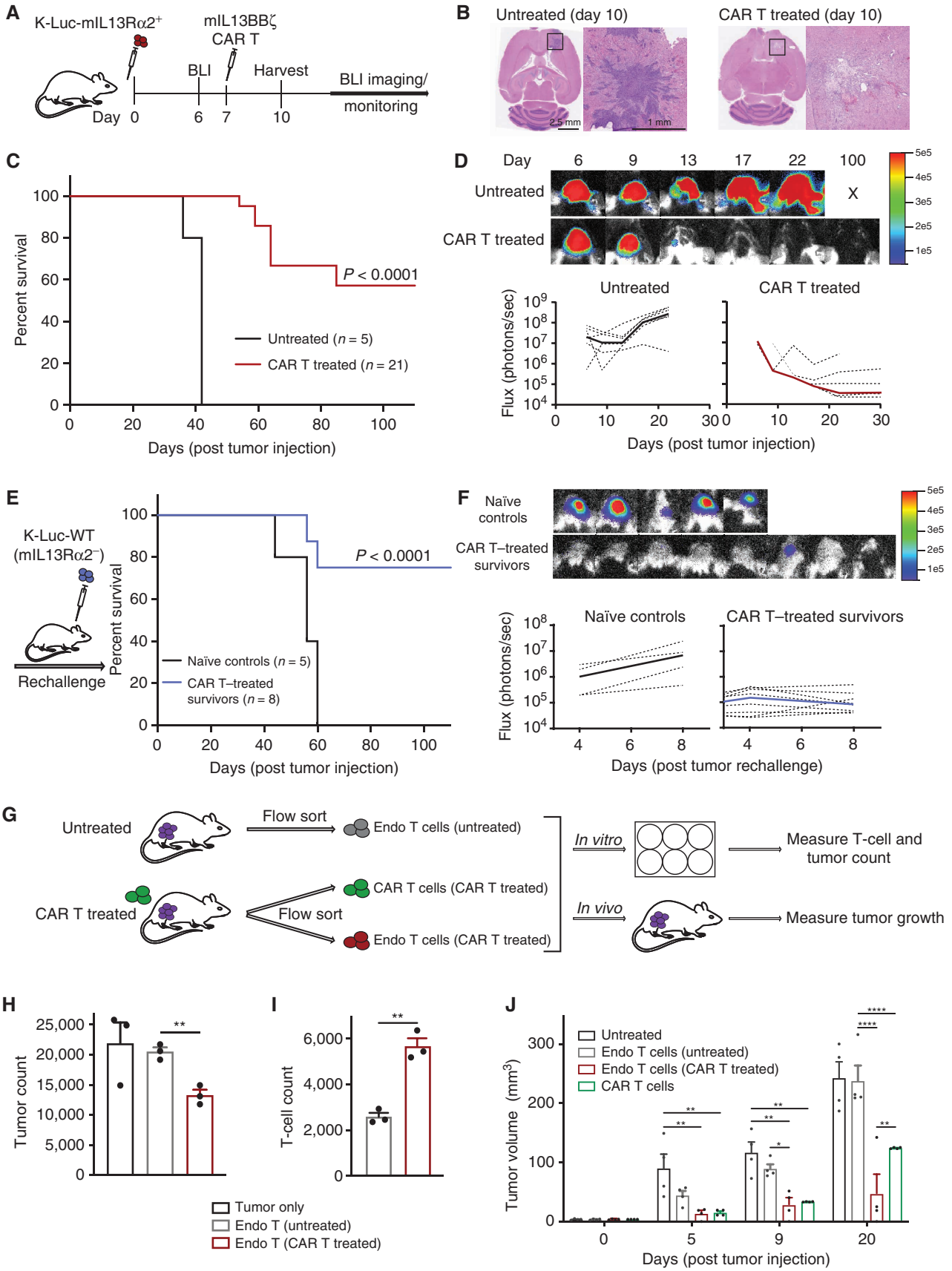

Published OnlineFirst April 9, 2021; DOI: 10.1158/2159-8290.CD-20-1661

immunologic memory in two independent tumor models with differential responsiveness to anti–PD-1 immunotherapy (27, 29). The capacity of CAR T cells to induce endogenous immunity against IL13Rα2-negative tumor cells again required a more established TME, as mice cured in the small tumor model (4-day engraftment before CAR T-cell therapy) were not capable of mounting antitumor responses following rechallenge with parental tumors (Supplementary Fig. S7A and S7B). Indeed, flow cytometry analysis of tumor-infiltrated T-cell and myeloid populations (Supplementary Fig. S8A) demonstrates an increased number of immune cells in the 7-day compared with the 4-day tumor model (Supplementary Fig. S8B and S8C). These results suggest that while CAR T-cell therapy is very effective in smaller tumors because of strong direct killing of antigen-positive tumor cells, it does not necessarily result in the establishment of endogenous immunity, and while "7-day model" is a larger tumor with an established TME that cannot be fully eliminated by CAR T cells in an antigen-dependent manner, the induction of host immunity can cooperate with CAR T-cell therapy to improve therapeutic effectiveness, resulting in surviving mice successfully rejecting antigen-negative tumors upon rechallenge, demonstrating that a memory immune response was effectively established. This observation also suggests that tumor exposure is not sufficient to induce endogenous antitumor immunity, and instead the establishment of immunologic memory requires both CAR T-cell therapy and the host immune infiltrates. In a similar set of experiments, we compared the antitumor activity of mIL13BBζ CAR T cells against IL13Rα2$^+$ K-Luc (100% IL13Rα2$^+$ cells) versus a mixture of IL13Rα2$^+$ K-Luc and IL13Rα2$^-$ parental K-Luc tumor cells (1:1 ratio; Supplementary Fig. S9A and S9B). Supporting the notion that CAR T cells can promote endogenous immune responses against antigen-negative tumor cells, mIL13BBζ CAR T cells mediated comparable survival benefit against tumors with homogenous and heterogeneous IL13Rα2 antigen expression (Supplementary Fig. S9C). Again, the response to IL13Rα2-negative tumors required a more established tumor microenvironment, as CAR T-cell therapy was less effective against mixed antigen tumors (1:1 ratio) in the small tumor model (day 4; $P < 0.001$; Supplementary Fig. S9D). Together, these observations suggest that the host immune cells within the TME cooperate with CAR T-cell therapy to augment antitumor responses and that CAR T cells can promote endogenous antitumor memory responses.

To directly evaluate whether CAR T-cell therapy can potentiate the generation of tumor-specific T cells, we isolated intratumoral endogenous (CD3$^+$CD19$^-$) and CAR T cells (CD3$^+$CD19$^+$) from untreated and CAR T cell–treated mice in the IL13Rα2$^+$ K-Luc glioma model (3 days post-treatment; Supplementary Fig. S10), either *ex vivo* cocultured with tumor cells or adoptively transferred into new tumor-bearing mice (Fig. 2G). Importantly, we find that endogenous T cells isolated from CAR T cell–treated tumors, but not T cells from untreated mice, exhibited enhanced killing of IL13Rα2$^+$ K-Luc tumors and T-cell proliferation in coculture assays [10:1, effector:target (E:T) ratio; 72 hours; Fig. 2H and I]. To assess *in vivo* function, endogenous T cells from untreated and CAR T cell–treated mice were isolated and adoptively transferred into IL13Rα2$^+$ K-Luc tumor-bearing mice. Measurement of tumor progression demonstrated that mice injected with endogenous T cells isolated from CAR T cell–treated mice showed a significant reduction in tumor growth compared with the control groups (Fig. 2J). Collectively, these results establish that CAR T cells have the potential to promote antigen spread and the generation of tumor-specific T-cell responses.

CAR T Cells Activate Innate and Adaptive Immune Subsets in the TME

To elucidate immune-related changes in the TME that coincide with the establishment of endogenous antitumor immunity following CAR T-cell therapy, we interrogated both the lymphoid and myeloid compartments by gene and protein expression profiling. Focusing first on the lymphoid compartment, we performed NanoString analysis of purified intratumoral CD3$^+$ cells and demonstrated a dramatic and global reshaping of the T-cell compartment at a transcriptome level in CAR T cell–treated mice compared with untreated mice (Fig. 3A). To increase resolution and more accurately define subpopulations, we performed single-cell RNA sequencing (scRNA-seq) on isolated CD45 cells from the brains of untreated or CAR T cell–treated mice (Supplementary Fig. S11A–S11C). We then computationally separated lymphoid and myeloid populations and reanalyzed the scRNA-seq data at higher granularity. This approach yielded nine distinct lymphoid subpopulations broadly defined by the distribution of classic marker genes, including three distinct subsets of CD8$^+$ T cells (CD8_L2, CD8_L3, and CD8_L4), two subsets of CD4$^+$ T cells (CD4_L1, CD4_L6), one subset of natural killer (NK) cells, two subsets of B cells, and one subset resembling γδT cells (Fig. 3B; Supplementary Fig. S11D). The frequency of CD8_L2 remained unchanged, but interestingly, post-CAR T-cell therapy, increased frequency of CD8_L3 and CD8_L4 subclusters was detected (Supplementary Fig. S11D). Focusing on T-cell subclusters, CD8_L3 is observed mainly

Figure 2. mIL13BBζ CAR T cells induce an endogenous immunologic memory response and generation of tumor-reactive T cells. **A,** Schematic of *in vivo* experimental design. **B,** Representative images of hematoxylin and eosin (H&E) staining show invasive K-Luc in untreated brains and tumor elimination in CAR T cell–treated brains. **C,** Survival curve of mice bearing K-Luc-mIL13Rα2$^+$ tumors in untreated and CAR T cell–treated groups. **D,** Representative bioluminescence (BLI) images (top) and flux values (bottom) show tumor growth in untreated and CAR T cell–treated groups. Individual mice are represented with dotted lines, while median flux is represented by the thick line. **E,** Survival of mice cured by CAR T-cell therapy and rechallenged with IL13Rα2-negative K-Luc tumors. **F,** Representative BLI images from day 8 post rechallenge tumor injection (top) and flux values (bottom) show tumor growth in naïve controls and survivors of CAR T-cell therapy groups. Individual mice are represented with dotted lines, while median flux is shown by the thick line. **G,** Overview of experimental design. *In vitro* killing (**H**) and expansion of endogenous T cells (**I**) isolated from untreated or CAR T cell–treated mice against K-Luc-mIL13Rα2$^+$ tumor cells (E:T, 10:1). **J,** Assessment of *in vivo* killing capacity of isolated CAR T cells and endogenous T cells from untreated or CAR T cell–treated cells in tumor (K-Luc-mIL13Rα2$^+$) bearing mice. Data are representative of at least two independent experiments. Data are presented as means ± SEM (**H**–**J**) and were analyzed by two-tailed, unpaired Student *t* test. Differences between survival curves (**C** and **E**) were analyzed by log-rank (Mantel–Cox) test. *, $P < 0.05$; **, $P < 0.01$; ***, $P < 0.001$; ****, $P < 0.0001$ for indicated comparisons.

Published OnlineFirst April 9, 2021; DOI: 10.1158/2159-8290.CD-20-1661

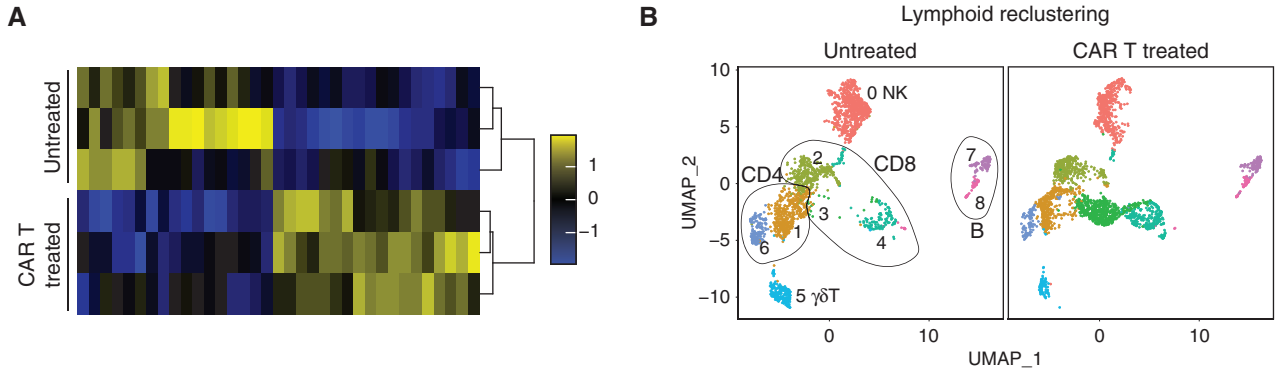

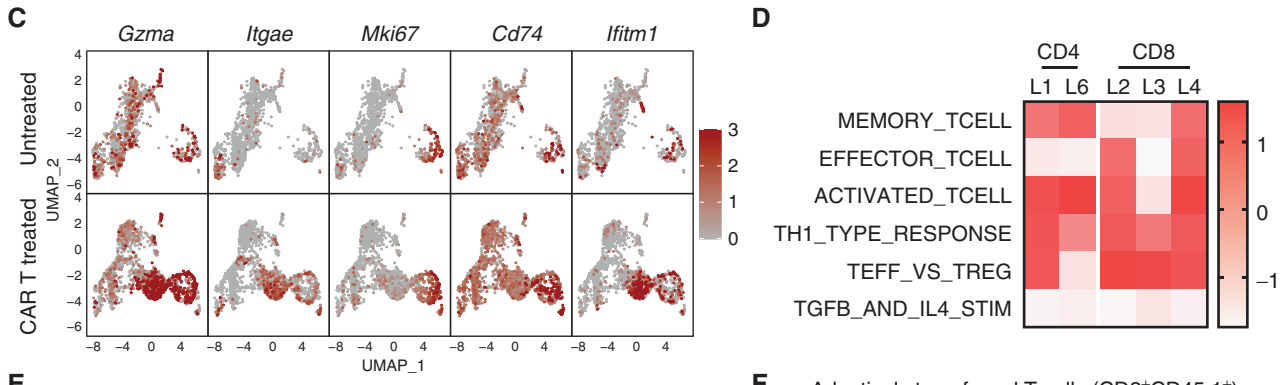

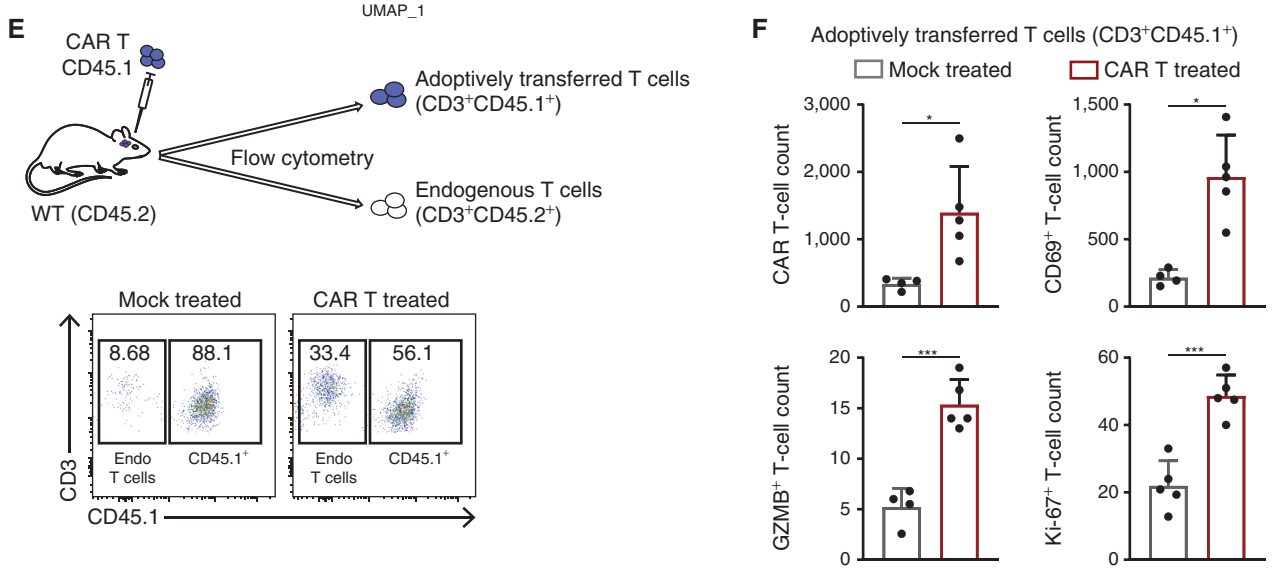

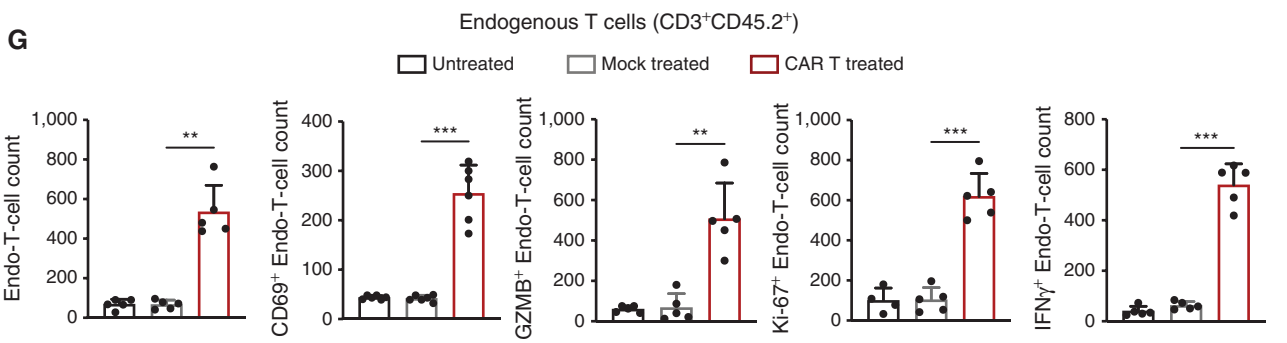

Published OnlineFirst April 9, 2021; DOI: 10.1158/2159-8290.CD-20-1661

posttherapy and is characterized by expression of *Cxcr3* (Supplementary Fig. S12A), which is associated with T-cell trafficking and expression of *Itgae* (CD103), *Cd74* (HLADR), and *Ifitm1* (IFN-induced transmembrane protein 1) that correspond to activated resident memory CD8 T-cell phenotype (Fig. 3C). CD8_L4 expanded posttherapy and was identified as highly activated, effector T cell based on higher expression of *Mki67* (Ki67), *Cd74*, and *Gzma* genes (Fig. 3C). Within the CD4 subsets, the frequency of CD4_L1 cluster remained unchanged after therapy, although posttherapy this cluster displayed a modest increase in expression of *Il7r, Tcf7*, and *Itga4* genes, which is associated with effector memory CD4 T cells (Supplementary Fig. S12A). Intratumoral Tregs, defined by subcluster CD4_L6 based on the expression of *Cd4*, *Foxp3*, *Tnfrsf18* (GITR), and *Ctla4*, decreased after CAR T-cell therapy (Supplementary Fig. S12B). Overall, gene set enrichment analysis (GSEA) revealed enrichment of gene signatures associated with activated and Th1 responses in most T-cell subclusters (Fig. 3D). Taken together, these studies reveal that CAR T cells can dramatically alter the lymphoid compartment within tumors and increase activated, memory, or effector T-cell populations.

To further characterize T-cell populations post–CAR T-cell therapy at cellular level and differentiate changes in endogenous versus adoptively transferred T cells, isogenically mismatched CD45.1 CAR T cells were used to treat IL13Rα2$^+$ K-Luc tumors engrafted in CD45.2 mice (Fig. 3E). Following intracranial delivery, CAR T cells (CD3$^+$CD45.1$^+$CD19$^+$), but not mock-transduced T cells (CD3$^+$CD45.1$^+$CD19$^-$), displayed a significant increase in T-cell count and expression in markers of activation (CD69$^+$), cytotoxic function (GZMB$^+$), and proliferation (Ki-67$^+$; Fig. 3F), establishing that the observed effector activity was CAR-dependent. Importantly, only after CAR T-cell therapy, a significant increase in the endogenous T-cell (CD3$^+$CD45.2$^+$) count with activated (CD69$^+$), proliferative (Ki-67$^+$), and cytotoxic (GZMB$^+$) phenotypes was observed, which was not detected in untreated or mock-treated controls (Fig. 3G). This was in line with qPCR analysis demonstrating upregulation of *Gzma, Gzmb*, and *Prf1* genes in intratumoral CD3$^+$ T cells after CAR T-cell therapy (Supplementary Fig. S13). These results establish that CAR T cells promote endogenous T-cell activation and expansion, and are consistent with our previous finding that endogenous intratumoral T cells isolated post-CAR T-cell therapy have antitumor activity (Fig. 2H and I).

We next evaluated changes in the innate myeloid cells, including microglia/macrophages, as they represent a dominant immune population in glioma tumors and have decisive role in glioma pathogenesis (30). Analysis of intratumoral myeloid populations at single-cell level identified 17 distinct myeloid subsets, which underwent a striking remodeling following CAR T-cell therapy (Fig. 4A; Supplementary Fig. S14).

While some macrophage/monocyte subpopulations decreased in frequency, other populations expanded and reshaped the TME. Seven major monocyte/macrophage (*Itgam* and *Cd68*), four microglia (*Tmem119* and *P2ry12*), four DC (*Itgax*), and two neutrophil (*S100a9*) subpopulations were identified (Supplementary Fig. S14). GSEA revealed enrichment of genes associated with IFNγ-stimulated macrophage and microglia in CAR T cell–treated groups (Fig. 4B). Assessment of the main myeloid populations (macrophage, microglia, and neutrophils) identified higher expression of genes associated with mature and IFNγ-activated macrophages as well as stimulated neutrophils (Fig. 4C), further confirming that resident innate immune cells have been exposed to IFNγ-mediated activation.

NanoString analysis of intratumoral microglia/macrophages (CD11b$^+$) from the TME 3 days post-CAR T-cell therapy showed enrichment of genes that mediate antigen processing and presentation (e.g., *H2-Ab1, H2-Aa, H2-Eb1*; Fig. 4D). Further analyses with scRNA-seq confirmed that the majority of macrophage/microglia subclusters may be involved in antigen processing and presentation (Fig. 4E). Assessing CAR T cell–mediated changes in resident microglia/macrophage populations by flow cytometry, we found an increased frequency of activated brain-resident macrophage/microglia cells (CD86$^+$, MHCI^{hi}, MHCII^{hi}) in CAR T cell–treated mice (Fig. 4F), which also corresponded to increased number of activated myeloid cells (Supplementary Fig. S15A). Assessment of myeloid compartment also revealed a significant increase in the frequency and number of M1-type macrophages as measured by IFNγ$^+$CD11b$^+$ cells (Fig. 4F; Supplementary Fig. S15A). Conversely, expression of M2-type macrophages (CD163/CD206) decreased in the TME after CAR T-cell therapy (Supplementary Fig. S15B). Collectively, these data show that CAR T-cell therapy changes the GBM immune landscape and activates the host innate and adaptive immune cells. These results also further reveal a major role for IFNγ in inducing activation of local immune cells.

Lack of IFNγ in CAR T Cells Impairs *In Vivo* Antitumor Activity and Activation of Host Immune Cells

Given that the myeloid cells constituted the largest population in the glioma TME (ref. 31; Supplementary Fig. S15B) and our scRNA-seq analysis identified gene signatures related to IFNγ stimulation within the macrophages and microglia subclusters (Fig. 4B), we reasoned that IFNγ produced by antigen-stimulated CAR T cells may play a role in modulating the activation of resident macrophage/microglia cells

Figure 3. CAR T cells activate endogenous T cells in glioma tumor microenvironment. **A,** NanoString analysis shows global changes in gene expression of intratumoral T cells (CD3$^+$) isolated from untreated or CAR T cell–treated mice 3 days posttherapy. **B,** UMAP plots depict changes in lymphoid compartments in the glioma TME after CAR T-cell therapy. **C,** Feature plots demonstrate phenotypic characterization of T-cell subclusters and enriched pathways within CD8 and CD4 T-cell subclusters posttherapy. **D,** Heat map of enrichment scores (GSEA) shows enriched pathways in T-cell subclusters. **E,** Experimental design demonstrating the adoptive transfer of CD45.1$^+$ mock or CAR T cells (top) and a representative flow cytometry analysis shows frequency of endogenous (CD3$^+$CD45.2$^+$) or adoptively transferred T cells (CD3$^+$CD45.1$^+$) in glioma TME (bottom). **F,** Bar graphs compare adoptively transferred mock (CD3$^+$CD45.1$^+$) or CAR T-cell (CD3$^+$CD45.1$^+$CD19$^+$) number and phenotypic characterization (CD69, Ki-67, and GZMB). **G,** Bar graphs compare endogenous T-cell (CD3$^+$CD45.2$^+$) numbers and phenotypic characterization (CD69, Ki-67, GZMB, and IFNγ) in untreated, mock, or CAR T cell–treated mice ($n = 5$ per group). Data are representative of at least two independent experiments. Data are presented as means ± SEM (**F** and **G**) and were analyzed by two-tailed, unpaired Student *t* test. *, $P < 0.05$; **, $P < 0.01$; ***, $P < 0.001$ for indicated comparison.

Published OnlineFirst April 9, 2021; DOI: 10.1158/2159-8290.CD-20-1661

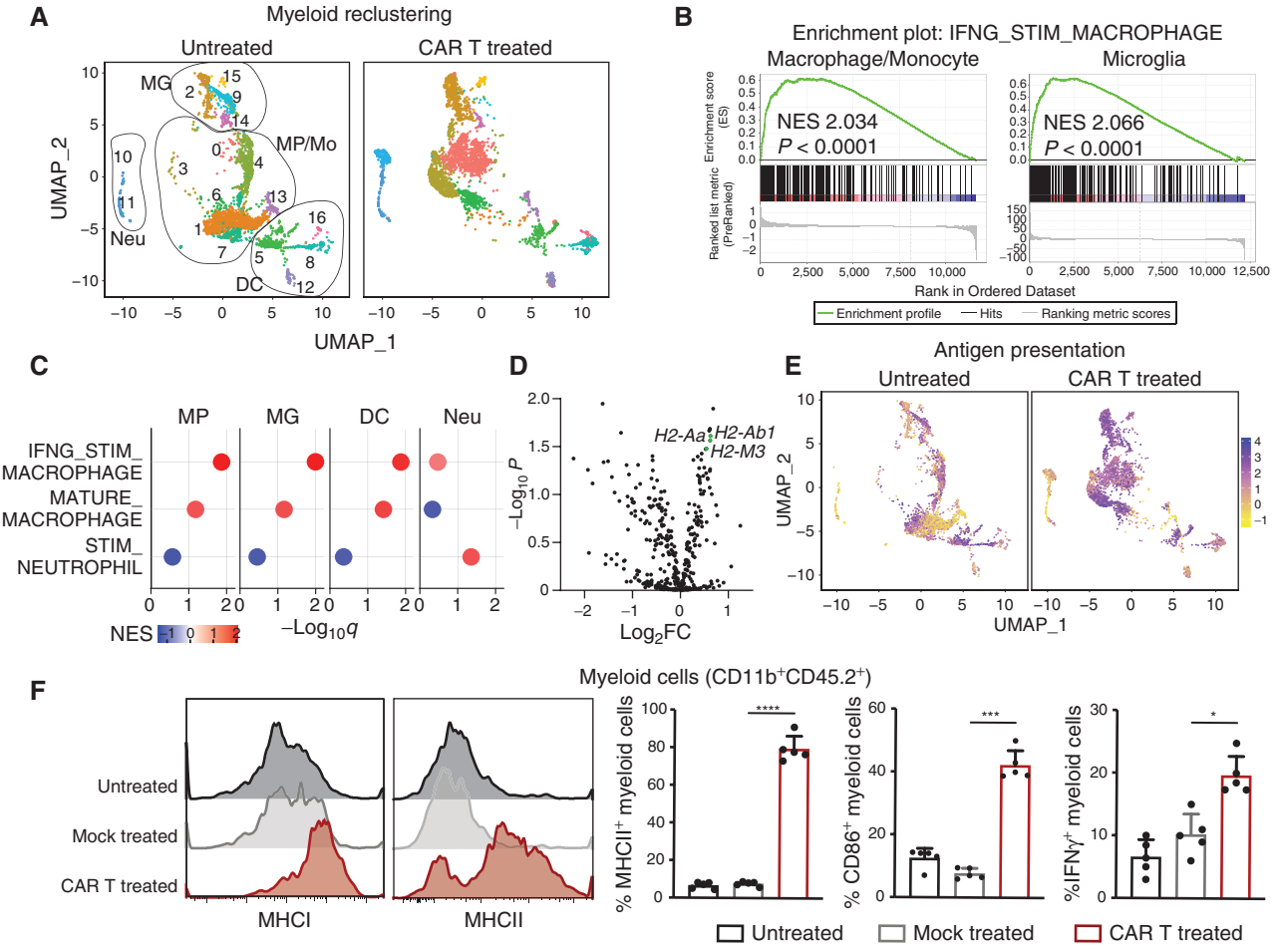

Figure 4. CAR T cells activate the resident myeloid population in glioma tumor microenvironment. **A,** UMAP plots of scRNA-seq depict changes in intratumoral myeloid cells from CAR T cell–treated or untreated mice (3 days posttherapy). **B,** Enrichment plot of IFNγ signaling pathways in intratumoral macrophage and microglia cells in CAR T cell–treated compared with untreated, as identified by the GSEA computational method. **C,** GSEA reveals upregulation of population-specific pathways in myeloid subclusters following CAR T-cell treatment. MP/Mo, macrophage/monocyte; MG, microglia; DC, dendritic cells; Neu, neutrophils. **D,** NanoString analysis show global changes in gene expression of myeloid cells (CD11b$^+$) isolated from CAR T cell–treated versus untreated mice. **E,** UMAP projections indicate relative expression levels of antigen presentation gene signatures at a single-cell level within the myeloid compartment. **F,** Representative flow cytometry histograms (left) and summary bar graphs (right) show intratumoral CD11b$^+$CD45.2$^+$ cells expressing MHCII, MHCI, CD86, and IFNγ. Data are presented as means ± SEM and analyzed by two-tailed, unpaired Student *t* test. *, $P < 0.05$; **, $P < 0.01$; ***, $P < 0.001$; ****, $P < 0.0001$ for indicated comparison.

and subsequent priming and induction of adaptive immune response.

IFNγ is one of the key effector cytokines abundantly produced by CAR T cells upon activation and is a prototypic macrophage activator (14). To investigate whether IFNγ secreted by CAR T cells is responsible for changes observed in phenotype and function of resident macrophages/microglia cells, CAR T cells were generated from wild-type (CAR T^{WT}) or *IFNγ−/−* (CAR T$^{IFNγ−/−}$) mice (Fig. 5A) and characterized accordingly. CAR transduction efficiency, cell viability, expansion in both CAR T-cell populations (CAR T^{WT} and CAR T$^{IFNγ−/−}$) showed comparable therapeutic products with some difference in ratio of CD4:CD8 T cells ($P < 0.05$; Fig. 5B). We next verified the functionality of CAR T cells derived from *IFNγ*$^{-/-}$ mice by conducting an *in vitro* killing assay in comparison with CAR T cells from WT mice, which demonstrated comparable killing potency at a 1:1 E:T ratio (Fig. 5C). Assessment of CAR T-cell polyfunctionality demonstrated comparable production of TNFα and GZMB in both CAR T^{WT} and CAR T$^{IFNγ−/−}$ cells with expected lack of IFNγ production in CAR T$^{IFNγ−/−}$ (Fig. 5D). *In vivo*, mice that received CAR T$^{IFNγ−/−}$ exhibited poor overall survival compared with mice treated with CAR T^{WT}, indicating that IFNγ deficiency in CAR T cells dampens their antitumor activity *in vivo* (Fig. 5E and F). Gene expression analysis of tumor and the associated TME 3 days post-CAR T-cell therapy revealed enhanced expression in genes involved in activation and proinflammatory cytokines in mice that received CAR T^{WT} cells and, conversely, reduced expression of genes involved in suppressive phenotype and function of intratumoral immune infiltrates (Fig. 5G), indicating that lack of IFNγ secretion by CAR T cells changes the glioma TME. IFNγ is a pleiotropic cytokine that induces activation of CD8 T cells (17), promotes polarization of Th1 CD4 cells (32), and reprograms or activates macrophage/microglia cells (14, 15). Therefore, we then

Published OnlineFirst April 9, 2021; DOI: 10.1158/2159-8290.CD-20-1661

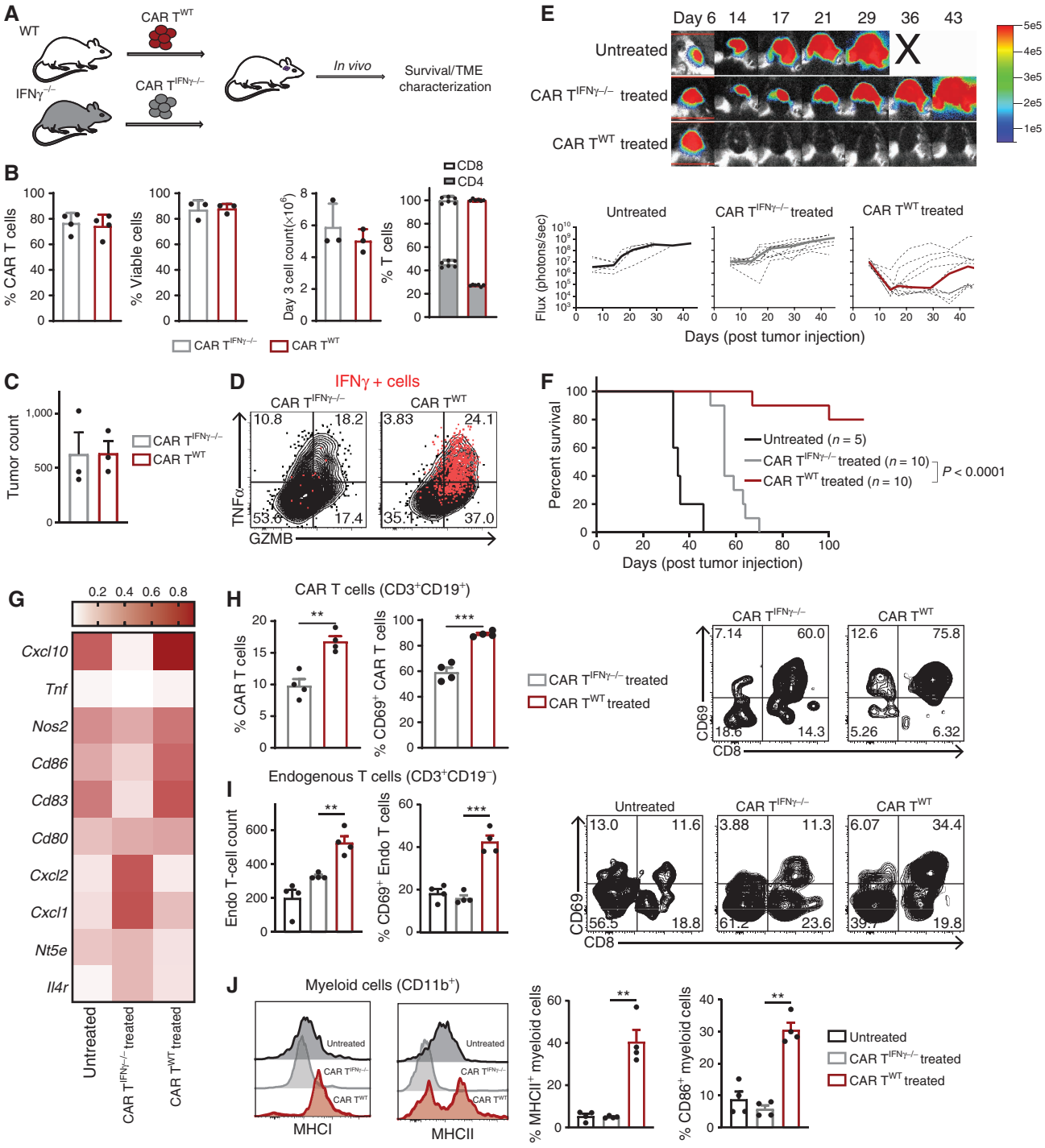

Figure 5. Lack of IFNγ production by CAR T cells impairs antitumor activity and activation of host immune cells. **A,** Schematic of the experimental design. **B,** Comparison of percent CAR positivity, viability, expansion, and CD4:CD8 ratio in CAR T^{WT} and CAR $T^{IFN\gamma-/-}$. **C,** *In vitro* killing of CAR T^{WT} and CAR $T^{IFN\gamma-/-}$ against K-Luc-mIL13Rα2+ cells (E:T, 1:1). **D,** Representative flow cytometry plot depicts intracellular cytokine levels (TNFα, GZMB, and IFNγ) in WT and IFNγ−/− CAR T cells after exposure to K-Luc-mIL13Rα2+ tumors. **E,** Representative bioluminescence (BLI) images (top) and flux values (bottom) show tumor growth in untreated, CAR T^{WT} or CAR $T^{IFN\gamma-/-}$. Individual mice are represented with dotted lines and median flux is shown in thick line. **F,** Survival curve of mice bearing K-Luc-mIL13Rα2+ tumors in untreated, CAR T^{WT}–treated and CAR $T^{IFN\gamma-/-}$–treated groups. **G,** Heat map indicates normalized expression of genes associated with immune activation and suppression in the TME. **H,** Bar graphs (left) and representative flow cytometry plots (right) comparing CAR T-cell ($CD3^+CD19^+$) number and activation phenotype (CD69). **I,** Bar graphs (left) and representative flow cytometry plots (right) comparing endogenous T-cell ($CD3^+CD19^-$) number and activation phenotype (CD69). **J,** Representative histograms (left) and bar graphs (right) showing phenotype in myeloid ($CD11b^+$) compartment. Data are representative of at least two independent experiments. Each symbol represents one individual (**H**–**J**). Data are presented as means ± SEM and were analyzed by two-tailed, unpaired Student *t* test. Differences between survival curves (**F**) were analyzed by log-rank (Mantel–Cox) test. *, $P < 0.05$; **, $P < 0.01$; ***, $P < 0.001$ for indicated comparison.

Published OnlineFirst April 9, 2021; DOI: 10.1158/2159-8290.CD-20-1661

assessed whether lack of IFNγ secreted by CAR T cells affected the host immune cells. Flow cytometry analysis of TME 3 days post-CAR T-cell therapy revealed a significant decrease in T-cell number, in both endogenous and CAR T cells, which correlated with a reduction in activated ($CD69^+$) T cells (Fig. 5H and I). Furthermore, a significant increase in frequency of $MHCI^+/MHCII^+$ and $CD86^+$ macrophage/microglia cell activation in tumor-bearing mice that received CAR T^{WT} compared with CAR $T^{IFN\gamma-/-}$ cells (Fig. 5J) was observed. Importantly, lack of IFNγ secretion by the CAR T cells resulted in higher M2-type intratumoral macrophages in mice that received CAR $T^{IFN\gamma-/-}$ cells compared with CAR T^{WT} cells (Supplementary Fig. S16). Thus, IFNγ production as a consequence of CAR T-cell antitumor activity resulted in activation and reinvigoration of T cells and reprogramming of macrophage/microglia cells to enhance their activation and antigen-presenting potential.

Lack of IFNγ Signaling in the Host Results in Dampened CAR T-cell Antitumor Activity *In Vivo*

Previous studies have reported IFNγ signaling as a signature of response to immunotherapies such as anti–PD-1 treatment (33). To investigate whether host IFNγ signaling plays a role in the CAR T cell–mediated immune response, CAR T^{WT} cells were adoptively transferred into K-Luc–bearing WT or *IFNγR*$^{-/-}$ mice (Fig. 6A). *IFNγR*$^{-/-}$ mice that received CAR T^{WT} cells demonstrated a survival disadvantage, suggesting that lack of IFNγ signaling in the host immune cells dampens the antitumor activity of CAR T cells and overall survival (Fig. 6B and C).

Gene expression analysis of TME 3 days post-CAR T-cell therapy, which includes tumor, tumor-associated immune and stroma cells, revealed that lack of IFNγ responsiveness in the host immune cells resulted in reduced expression of genes involved in activation and proinflammatory responses (*Cd40, Nos2, Tnfα, Gzma, Gzmb, Prf1,* and *Ifnγ*; Fig. 6D). To further investigate CAR T cell–mediated changes in the immune landscape, we adoptively transferred isogenically mismatched ($Thy1.1^+$) CAR T^{WT} cells into K-Luc–bearing WT or *IFNγR*$^{-/-}$ mice. Flow cytometry analysis of immune subsets in the TME revealed a significant increase in activated macrophage/microglia cells ($CD86^+$ and $MHCII^+$) and M1 markers ($IFN\gamma^+TNF\alpha^+$) and a decrease in M2 markers ($CD163^+CD206^+$) in WT compared with *IFNγR*$^{-/-}$ mice 3 days post-CAR T-cell therapy (Fig. 6E; Supplementary Fig. S17A and S17B). Compared with WT mice, the number of endogenous T cells ($Thy1.2^+CD3^+$), activated with proliferative and effector cytokine–producing capacities, was significantly lower in *IFNγR*$^{-/-}$ mice (Fig. 6F). Lower frequency of regulatory T cells ($CD4^+CD25^+FOXP3^+$) and higher effector-type T cells ($CD8^+GZMB^+$) were detected in WT mice that received CAR T cells as compared with *IFNγR*$^{-/-}$ CAR T cell–treated groups (Supplementary Fig. S18A–S18C). Furthermore, a significant increase in exhausted T cells was observed in *IFNγR*$^{-/-}$ compared with WT host at a later time point after CAR T-cell therapy, (Supplementary Fig. S18D). Interestingly, higher levels of adoptively transferred CAR T cells ($Thy1.1^+CD3^+$) were detected in WT mice, and these T cells were more proliferative ($Ki\text{-}67^+$) and cytotoxic ($IFN\gamma^+$ and $GZMB^+$) relative to *IFNγR*$^{-/-}$ mice (Fig. 6G), suggesting IFNγ-dependent positive feedback from host immune cells that promotes CAR T-cell activity in the TME. Collectively, these results confirm that there is an interplay between host and adoptively transferred immune cells and that host IFNγ signaling in the glioma TME is necessary for mounting a potent immune response during CAR T-cell therapy.

Human CAR T-cell Therapy Modulates Patient Host Immune Cells

To evaluate the clinical relevance of IFNγ signaling for human CAR T-cell therapy, we next investigated the impact of CAR T-cell antitumor activity on human endogenous immune cells in patients with GBM. To assess whether CAR T cells are able to promote activation of GBM patient monocytes or macrophages, we developed an *in vitro* assay to phenotypically characterize patient myeloid populations in the presence of CAR T-cell antitumor activity. Conditioned media (CM) from coculture of human CAR T cells and patient-derived glioma tumor lines were collected and subsequently incubated with glioma patient–derived monocytes (Supplementary Fig. S19A), *ex vivo* differentiated patient macrophages, or total $CD3^+$ patient T cells (Fig. 7A). Phenotypic and morphologic assessments revealed that CM from CAR T plus tumor coculture promoted differentiation and activation of patient-derived monocytes and macrophages, as demonstrated by an increase in expression of activation markers ($CD14^+CD86^+/CD80^+$ and $CD14^+HLADr^+$; Fig. 7B–D; Supplementary Fig. S19B and S19C). Gene analysis demonstrated increased expression of genes associated with classic M1 macrophages (Fig. 7E; Supplementary Fig. S19D). Accordingly, exposure to CM from CAR T plus tumor coculture resulted in induced activation of isolated T cells from GBM patient blood, as evidenced by increased expression of CD69 (Fig. 7F and G). Importantly, blockade of IFNγ signaling in macrophages and T cells resulted in reduced activation (Fig. 7B–F), highlighting the impact of IFNγ in the CAR T cell–mediated activation of host immune cells in patients with GBM. Taken together, these findings suggest that IFNγ secreted by CAR T-cell antitumor function promotes polarization of monocytes into activated macrophages, further induces activation of differentiated macrophages, and promotes T-cell activation. These findings confirm our preclinical studies that an effective CAR T-cell therapy has the potential to stimulate the host immune cells and highlights the important roles that both IFNγ signaling and the host immune cells play in a successful CAR T-cell treatment.

DISCUSSION

Delineating the mechanisms that positively modulate host antitumor immunity is critical for the development of cancer immunotherapy. Our studies indicate that, in addition to direct antitumor activity toward malignant cells, CAR T cells have immune-stimulatory effects that result in activation of host innate immune subsets and subsequent engagement of adaptive immunity. We find that IFNγ signaling, both in CAR T cells and host, tightly controls adaptive and innate immunity. We employed well-characterized syngeneic glioma models to address fundamental questions about the role of resident immune cells in the glioma TME during the CAR T cell–mediated antitumor responses. The rationale for this study was based on our clinical observations, in which a patient with multifocal GBM had a CR to

Published OnlineFirst April 9, 2021; DOI: 10.1158/2159-8290.CD-20-1661

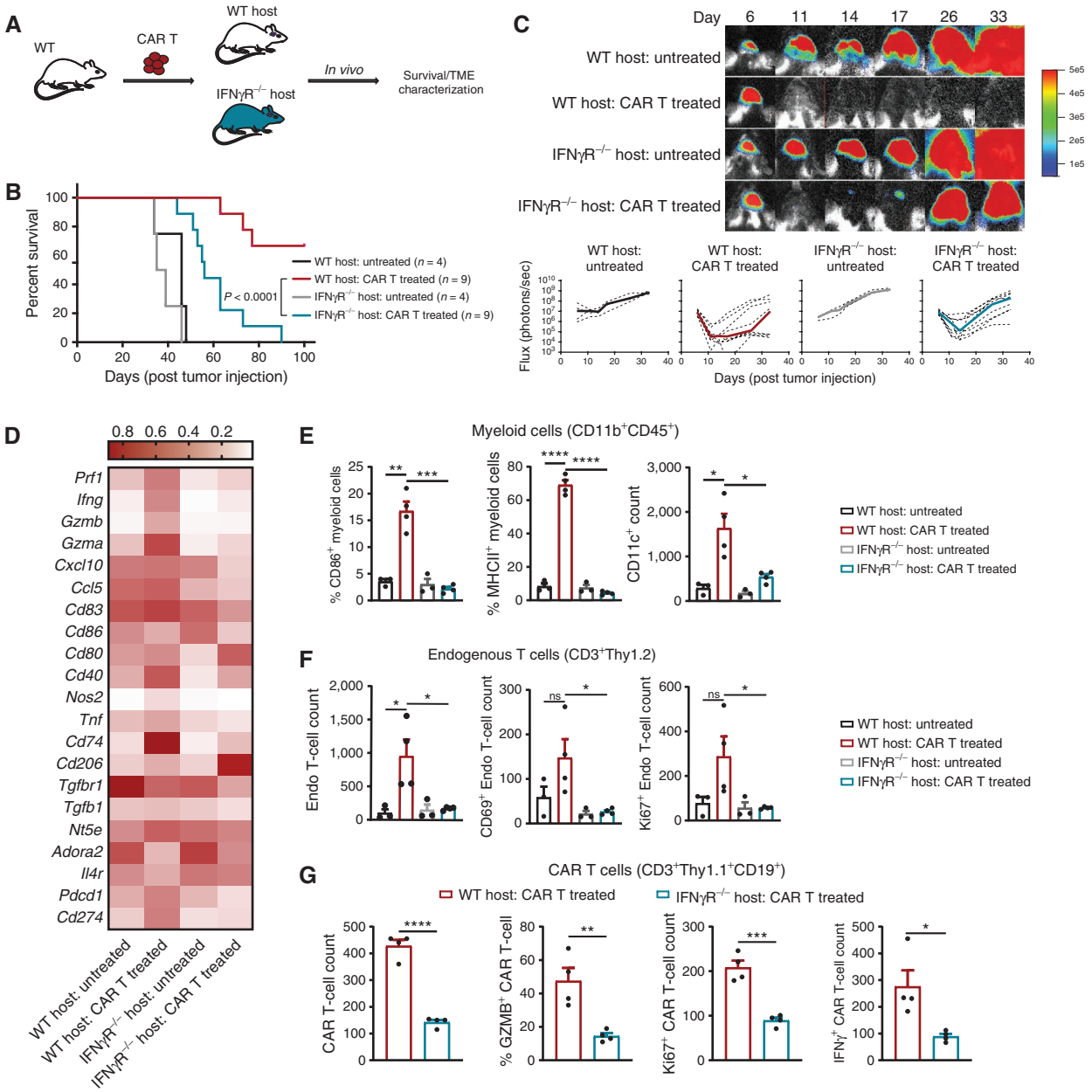

Figure 6. CAR T-cell therapy is impaired in IFNγR$^{-/-}$ tumor-bearing host. **A,** Schematic of the experimental design. **B,** Survival curve of mice bearing K-Luc-mIL13Rα2^{+} tumors in untreated or CAR T cell–treated in WT host or IFNγR$^{-/-}$ host. **C,** Representative bioluminescence (BLI) images (top) and flux values (bottom) show tumor growth. Individual mice are represented with dotted lines, while median flux is represented by the thick line. **D,** Heat map indicating normalized expression of genes associated with immune activation or suppression in the TME. **E,** Bar graphs of myeloid cells (CD11b^{+} CD45^{+}) show phenotypic changes (CD86, MHCII, and CD11c). **F,** Bar graphs of endogenous T cells (CD3^{+}Thy1.2) show changes in T-cell count, CD69, and Ki-67. **G,** Bar graphs of CAR T cells (CD3^{+}Thy1.1^{+}CD19^{+}) demonstrate changes in number, GZMB, Ki-67, and IFNγ. Data are representative of at least two independent experiments. Each symbol represents one individual mouse. Data are presented as means ± SEM (**E–G**) and were analyzed by two-tailed, unpaired Student *t* test. Differences between survival curves (**B**) were analyzed by log-rank (Mantel–Cox) test. *, $P < 0.05$; **, $P < 0.01$; ***, $P < 0.001$; ****, $P < 0.0001$ for indicated comparison.

IL13Rα2–CAR T-cell therapy despite the heterogeneous expression of IL13Rα2 on the tumors. This study provides insights into the immunologic signatures required for an effective anti-glioma CAR T-cell therapy, revealing that: (i) CAR T cells can activate host immune cells and induce tumor-specific T cells; (ii) mice cured from CAR T-cell therapy are immunized against antigen-negative tumors; (iii) effective CAR T-cell antitumor activity is dependent on IFNγ signaling, including both IFNγ secretion by CAR T and IFNγ signaling in host immune cells; (iv) clinically, IFNγ-dependent activation of patient host immune cells and generation of tumor-specific T cells can be induced by CAR T-cell therapy.

The GBM microenvironment is characterized by high numbers of myeloid cells and lower T-cell counts (31). Identifying mechanisms that regulate the activation of microglia/macrophages and/or increase the number of T cells in the

Published OnlineFirst April 9, 2021; DOI: 10.1158/2159-8290.CD-20-1661

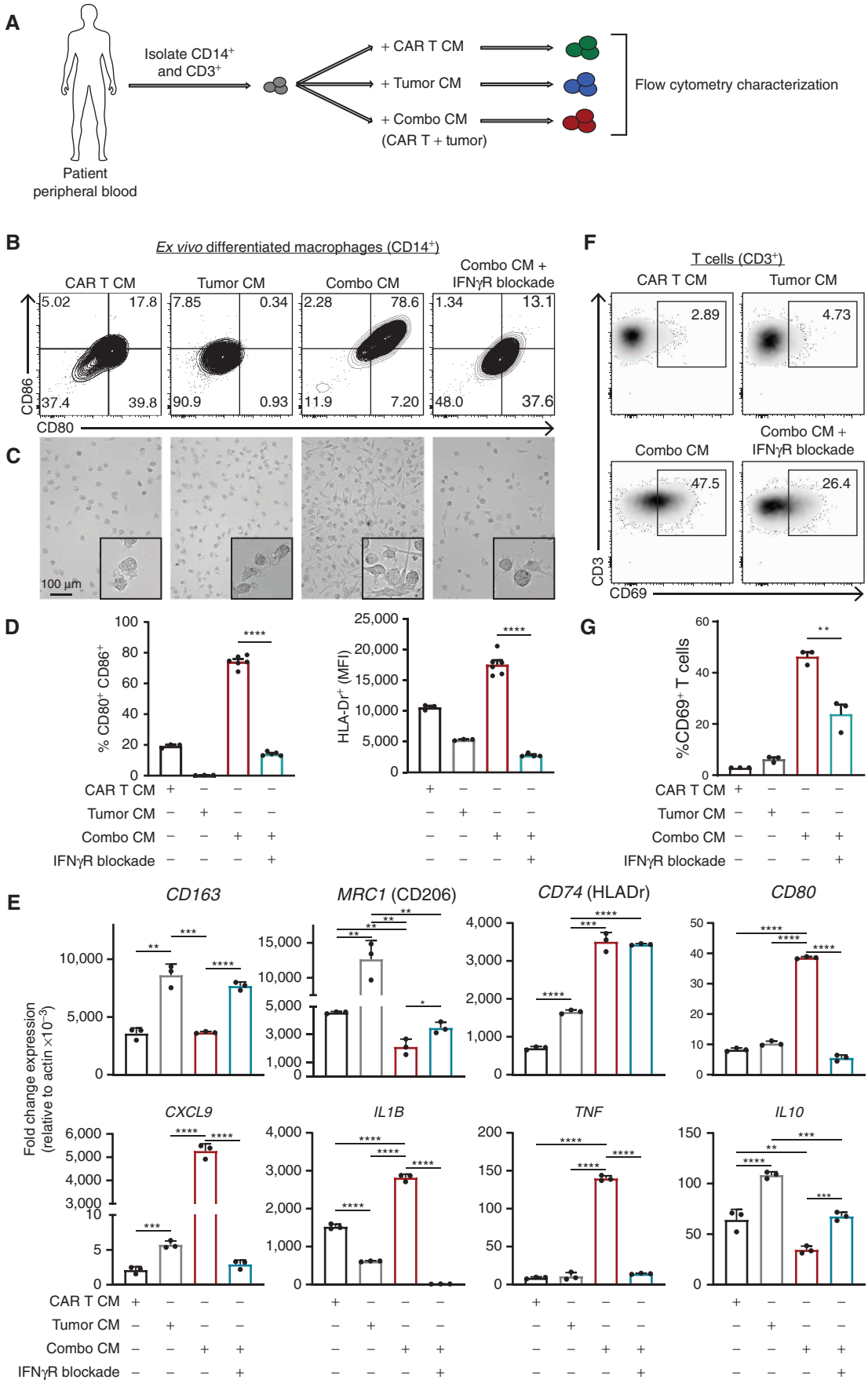

Published OnlineFirst April 9, 2021; DOI: 10.1158/2159-8290.CD-20-1661

TME are emerging strategies to overcome the immunosuppressive nature of GBM (34). We demonstrate that optimal CAR T-cell therapy can activate host immune cells, resident microglia/macrophages, and T cells. Accordingly, we also show that after CAR T-cell therapy, the resident microglia/macrophage subpopulations displayed gene expression patterns with enhanced antigen-presenting capacity. These findings are in line with recent studies demonstrating that lack of response in human solid tumors is due to not only the presence of exhausted CD8 T cells or overexpression of PD-L1 in tumors, but also the failure of T cells to interact with antigen-presenting myeloid populations in intratumoral niches (35). An important initiator of the immune response is antigen presentation with MHC proteins, and accordingly our findings strongly suggest that the presence of myeloid subpopulations with antigen-presenting phenotype is important in the CAR T cell–mediated antitumor immune response.

We also show evidence for an increase in the number of endogenous T cells after CAR T-cell therapy. This may be due to increased proliferation of existing T cells or an increase in T-cell infiltration. The elevated number of endogenous Ki-67$^+$ T cells and presence of *Mki67*-expressing subclusters may point toward potential proliferation of existing T cells in the TME. Detection of CD8$^+$ lymphoid subclusters with higher *Cxcr3* expression post-CAR T-cell therapy, however, also support increased infiltration of CD8 T cells. It should be noted that, in line with previous studies (35), the reduction in intratumoral CD4$^+$ Tregs and reduction in the Treg subcluster after CAR T-cell therapy indicate a reduction in suppressive factors in the TME. Our finding that the surviving mice post-CAR T-cell therapy rejected the antigen-negative tumor cells validates the notion that CAR T cells mediate changes in immune landscape and subsequently induce endogenous memory response.

To investigate potential mechanisms of CAR T cell–mediated antitumor activity, we identified IFNγ as a major player in activation of the host immune cells in glioma TME. IFNγ, a key cytokine secreted by activated CAR T cells, is involved in inducing innate and adaptive immunity (14, 16, 33, 36). IFNγ is critical in activation of macrophages (14, 35) and microglia cells (15), and induction of memory alveolar macrophages post viral infection (37). IFNγ is also involved in recruitment and activation of cytotoxic T cells, polarization of CD4$^+$ T cells into Th1 effector cells, and reduction of tumor-promoting Treg development and function (16–18). These findings support our observation that IFNγ is a critical cytokine with important roles in driving CAR T cell–associated effects on the endogenous TME within solid tumors, priming innate and adaptive immunity components against tumor cells and conferring long-lasting antitumor immunity.

While persistent IFNγ signaling paradoxically is linked to inhibitory feedback circuits through tumor cells and immune cells, known as "adaptive resistance," the IFNγ-mediated responses are still positively associated with patient survival in several cancers (16, 38). Upregulation of cell surface MHC class I by IFNγ is crucial for host response to intracellular pathogens and tumor cells. IFNγ also upregulates cell surface MHC class II on antigen-presenting cells. Thus, in the early phase of antigen recognition and the interaction between adaptive and innate immune cells, IFNγ responses are key to engage the innate and adaptive arms for a potent CAR T-cell therapy in GBM. While this study highlights the importance of IFNγ, our current results do not exclude other potential mechanisms of induction of host immune response, including tumor immune landscape and other inflammatory cytokines. These findings outline the adjuvant potential of CAR T cells that drives the generation of antitumor immune responses and endogenous memory responses.

Clinically, CAR T-cell responses in GBM and other solid tumors have been inadequate for most patients. The heterogeneous nature of solid tumors and the suppressive TME create significant challenges for CAR T-cell therapy. Furthermore, long-lasting antitumor immunity in patients is oftentimes not observed, likely due to evolution of the tumor under immune pressure leading to immune evasion (39). What will it take to improve CAR T-cell response rates for solid tumors? This study highlights the importance of the immunomodulatory effects of CAR T-cell therapy, through production of inflammatory cytokines. Our findings are supported by clinical examples of productive CAR T-cell responses in solid tumors. We have previously reported that IL13Rα2-CAR T cell–mediated CR in a patient with GBM was associated with increases in inflammatory cytokines and activated endogenous immune cells in the cerebrospinal fluid (20). Likewise, a recent study reported evidence of endogenous immune reactivity after HER2–CAR T-cell therapy, which correlated with a positive patient response (21). These findings suggest that tumor-dependent characteristics (i.e., tumor mutational burden and IFNγ responsiveness) and features of the TME (i.e., CD3 infiltration) may affect CAR T-cell responsiveness. Therefore, improving the effectiveness of CAR T-cell therapy more broadly for solid tumors may require additional strategies to enhance the induction of host antitumor responses (8, 13, 40, 41).

In conclusion, this report highlights the interplay between CAR T cells and the host immune cells in GBM. It is the first report that underlines the adjuvant potential of CAR T cells and the importance of host innate and adaptive immune cells in the context of CAR T-cell therapy for solid tumors. Our findings provide mechanistic evidence that CAR T cell, a potent antitumor agent, functions as an immunomodulatory adjuvant therapy that engages resident innate immune populations and generates tumor antigen–specific cytotoxic T cells. These insights strongly support the need to consider targeting/engaging both innate (e.g., macrophages) as well as adaptive (CD4$^+$ and CD8$^+$ T cells) immunity to improve the efficacy of

Figure 7. CAR T cells can activate GBM patient immune cells through the IFNγ pathway. **A,** Schema of experimental design. Representative flow cytometry (**B**), microscopy images (**C**), and bar graph summary (**D**) of phenotypic changes of patient macrophages after incubation in conditioned media (CM) collected from unactivated T cells (CAR T CM), tumor only (Tumor CM) versus tumor-activated CAR T cells (Combo CM), or tumor-activated CAR T cells with IFNγR blockade. **E,** qPCR analysis shows genes associated with macrophage activation after incubation in condition media as described in **B**–**D**. Representative flow cytometry (**F**) and bar graph summary (**G**) of phenotypic changes in patient T cells after incubation in conditioned media as described in **B**–**D**. Each symbol represents one replicate. Data are presented as means ± SEM (**D**, **E**, and **G**) and were analyzed by two-tailed, unpaired Student *t* test. *, $P < 0.05$; **, $P < 0.01$; ***, $P < 0.001$; ****, $P < 0.0001$ for indicated comparison.

Published OnlineFirst April 9, 2021; DOI: 10.1158/2159-8290.CD-20-1661

CAR T-cell therapy for solid tumors. Our work advances the biological understanding of the multifunctional aspect of CAR T-cell therapy with tremendous potential to incorporate novel therapeutic strategies for patients with this devastating cancer. Such immune engagement and cytotoxic T-cell initiation is desirable for current immunotherapies and would conceivably complement other modalities, including immune checkpoint blockade or immune-stimulatory adjuvant therapies.

METHODS

Mice and Cell Lines

C57BL/6/J, CD45.1 (B6.SJL-*Ptprc*^{a}*Pepc*^{b}/BoyJ), Thy1.1 (B6.PL-*Thy1*^{a}/CyJ), *IFNγR*$^{-/-}$ (B6.129S7-*Ifngr1*^{tm1Agt}/J), and *IFNγ*$^{-/-}$ (B6.129S7-*Ifng*^{tm1Ts}/J) mice were purchased from The Jackson Laboratory. NSG mice were bred at City of Hope (Duarte, CA). All mouse experiments were approved by the City of Hope Institutional Animal Care and Use Committee (IACUC).

The luciferase-expressing murine GL261 (GL261-Luc) and KR158B (K-Luc) glioma cells were transduced with lentivirus to produce murine IL13Rα2 (mIL13Rα2)-expressing sublines (GL261-Luc-mIL13Rα2 and K-Luc-mIL13Rα2). These tumor lines were maintained in DMEM (Gibco) supplemented with 10% FBS (Hyclone Laboratories), 25 mmol/L HEPES (Irvine Scientific), and 2 mmol/L L-glutamine (Lonza). Cell surface expression of mIL13Rα2 was authenticated by flow cytometry and immunofluorescence imaging.

Patient-derived glioma cells (PBT030, UPN109, and UPN097) were isolated from GBM patient resections under protocols approved by the City of Hope Institutional Review Board (COH IRB) and maintained as described previously (20). All tumor lines were authenticated for the desired antigen/marker expression by flow cytometry and the cells were tested for *Mycoplasma* and maintained in culture for less than 1–3 months.

CAR T-cell Production

Human CAR T Cells. Naïve and memory T cells were isolated from healthy donors at City of Hope under protocols approved by the COH IRB (6, 42). The construct of IL13Rα2-targeted CAR and CAR transduction was described in previous studies (6, 7, 20). In brief, primary T cells were stimulated with Dynabeads Human T expander CD3/CD28 (Invitrogen; T cells: beads = 1:3) for 24 hours and transduced with CAR lentivirus [multiplicity of infection (MOI) = 0.3]. Seven days after CAR transduction, CD3/CD28 beads were removed and cells were resuspended and expanded in X-VIVO 15 media (Lonza) containing 10% FCS, 50 U/mL recombinant human IL2 (Novartis), and 0.5 ng/mL recombinant human IL15 (CellGenix) for additional 10–15 days before cryopreservation.

Murine CAR T Cells. The murine IL13Rα2 CAR was constructed in a MSCV retroviral backbone (Addgene), containing the extracellular murine IL13 and murine CD8 hinge, murine CD8 transmembrane domain, and intracellular murine 4-1BB costimulatory and murine CD3ζ signals. Following a T2A ribosomal skip, a truncated murine CD19 was inserted as a transduction marker. The resulting plasmid was transfected into PlatE cells (a gift from Dr. Zuoming Sun's lab) using Fugene (Promega). After 48 hours, the supernatant was collected and filtered using an 0.2-μm filter. The retroviral supernatant was aliquoted and frozen until the time of transduction.

Murine T cells were isolated from spleens of naïve C57BL/6J mice or appropriate strain (CD45.1, Thy1.1, or *IFNγ*$^{-/-}$) with EasySep Mouse T cell Isolation Kit (STEMCELL Technologies) and stimulated with Dynabead Mouse T-Activator CD3/CD28 beads (Gibco) at a 1:1 ratio. T cells were transduced on RetroNectin-coated plates (Takara Bio) using retrovirus-containing supernatants (described above). Cells were then expanded for 4 days in RPMI 1640 (Lonza) supplemented with 10% FBS (Hyclone Laboratories), 55 mmol/L 2-mercaptoethanol (Gibco), 50 U/mL recombinant human IL2 (Novartis), and 10 ng/mL recombinant murine IL7 (PeproTech). Before *in vitro* and *in vivo* experiments, the beads were magnetically separated from the T cells and CAR expression was determined by flow cytometry.

In Vivo Studies

All mouse experiments were performed using protocols approved by the City of Hope IACUC. Orthotopic GBM models were generated as previously described (43). Orthotopic tumor model was established by stereotactically implanting 1×10^5 tumor cells intracranially (i.c.) into the right forebrain of 8- to 10-week-old C57BL/6J, *IFNγR*$^{-/-}$, or NSG mice. Engraftment was verified by bioluminescence imaging one day prior to CAR T-cell injection. Mice were randomized into groups based on bioluminescence signal. Investigators were not blinded for randomization and treatment. Four or seven days after tumor injection, mice were treated intracranially with 1×10^6 mIL13BBζ–CAR T cells. Tumor burden was monitored with SPECTRAL LagoX (Spectral Instruments Imaging) and analyzed using Aura software (v2.3.1, Spectral Instruments Imaging). Survival curves were generated by GraphPad Prism Software (v8).

For rechallenge experiments, clearance of tumor was verified by bioluminescence imaging prior to tumor rechallenge, where mice were injected with 10^4 K-Luc or 5×10^4 GL261-Luc cells.

For subcutaneous studies, 1×10^6 K-Luc-mIL13Rα2 in PBS was injected into the right and left flanks of 8–10-week-old C57BL/6J donor mice. Tumors were allowed to establish for 8 days, then 1×10^6 CAR T cells were injected directly into the tumor. Three days later, the tumor mass was harvested, manually dissociated, and sorted by flow cytometry into $CD3^+CD19^-$ (endogenous T cells) or $CD3^+CD19^+$ (CAR T cells) using the BD AriaSORP (BD Biosciences). The purified T-cell populations were either used as effector cells in *in vitro* coculture 10:1 (E:T) ratio as described below or reinjected back into 5-day-old subcutaneous K-Luc-mIL13Rα2 tumors, and tumor volume was measured over time using calipers.

Mice were also monitored by the Center for Comparative Medicine at City of Hope for survival and any symptoms related to tumor progression, with euthanasia applied according to the American Veterinary Medical Association Guidelines.

In Vitro Cytotoxicity

For the assessment of CAR T-cell proliferation and cytotoxic activity, K-Luc-mIL13Rα2 or GL261-Luc-mIL13Rα2 tumor cells were cocultured with murine CAR T cells at 1:3 CAR^+:tumor ratio for 48 hours. For coculture using effector T cells primed *in vivo*, T cells were plated at a 10:1 effector:tumor ratio for 72 hours. Cells were stained with anti-CD3, CD8, and CD19. Absolute number of viable tumor and CAR T cells was assessed by flow cytometry.

For the degranulation assay, CAR T cells and tumor cells were co-cultured at 1:1 effector:tumor ratio for 5 hours in the presence of GolgiStop Protein Transport Inhibitor (BD Biosciences). The cell mixture was stained with anti-CD3, CD8, and CD19 followed by intracellular staining with anti-IFNγ (BD Biosciences), GZMB, and TNFα (eBiosciences) antibodies and analyzed by flow cytometry.

All samples were acquired on MACSQuant Analyzer (Miltenyi Biotec) and analyzed with FlowJo software (v10.7) and GraphPad Prism (v8).

Patient Sample Analysis

CM was generated by seeding patient-derived glioma cells, human CAR T cells, or the combination at a 1:1 ratio for 24 hours. The supernatant was collected and centrifuged to remove any cell debris. Peripheral blood from male and female patients with GBM (obtained from scheduled blood draws under clinical protocols approved by the City of Hope) was lysed with PharmLyse buffer (BD Biosciences). CD3 and CD14 cells were isolated using selection kits (STEMCELL Technologies). CD14 and CD3 positive cells were incubated with CM,

Published OnlineFirst April 9, 2021; DOI: 10.1158/2159-8290.CD-20-1661

in the presence or absence of IFNγR neutralizing antibody (10 ng/mL; R&D Systems). For macrophage differentiation, CD14 cells were incubated in the presence of M-CSF (20 ng/mL; BioLegend) for 7 days and then exposed to CM, in the presence or absence of IFNγR neutralizing antibody (R&D Systems). After 48 hours, cells were visualized using Keyence microscope (Keyence), phenotyped by flow cytometry, and lysed for qPCR analysis.

Assessment of endogenous response in the unique responder (20) and a nonresponder patient to CAR T therapy was conducted as previously reported (44). Briefly, T cells were isolated from total peripheral blood before and during therapy. Every two days, T cells were incubated with irradiated (40 Gy) autologous tumor cells in the presence of IL2 (50 U/mL). After 14 days, T cells were purified and counted. T cells were cultured with fresh autologous tumor or irrelevant tumor line at a 10:1 (E:T) ratio and after 3 days, tumor counts were measured. IFNγ production was measured by stimulating the T cells with cell stimulation cocktail for an additional 4 hours followed by flow cytometry for intracellular IFNγ.

Flow Cytometry Assays

Human tumor cells were stained with IL13Rα2 (BioLegend) and human monocyte/macrophages were stained with CD14, CD80, CD86 (BD Biosciences) HLA-Dr (eBioscience). All samples were run on MACSQuant (Miltenyi Biotec).

Mouse tumor cells expanded *in vitro* were stained with an unconjugated goat anti-mouse IL13Rα2 (R&D Systems) followed by secondary donkey anti-goat NL637 (R&D Systems). Live murine CAR T cells were stained with CD8 (BioLegend), CD3, CD4, CD62L (eBioscience), or CD45RA (BD Biosciences). CD19 (BD Biosciences) was used as a surrogate to detect the CAR.

Brains from euthanized mice were removed at the indicated timepoints, and a rodent brain matrix was used to cut along the coronal and saggital planes to obtain a 4 × 4 mm section, centered around the injection site. These sections were minced manually, then passed through a 40 μm filter. Myelin was removed using Myelin Removal Beads II and LS magnetic columns (Miltenyi Biotec) according to the manufacturer's instructions, then cells were counted. Cells were stained and analyzed using MACSQuant (Miltenyi Biotec). For flow sorting, cells were stained and sorted using BD AriaSORP (BD Biosciences). For gene expression analysis of TME, the remaining cells were lysed for RNA. Each experiment was repeated independently at least twice. List of all antibodies (mouse and human) is provided in Supplementary Table S1.

Immunofluorescence and IHC

For immunofluorescence, K-Luc and GL261-Luc parental or mIL13Rα2-transduced cells were cultured on coverslip, stained with unconjugated goat anti-mouse IL13Rα2 (R&D Systems) followed by secondary donkey anti-goat NL557 (R&D Systems), and actin. Slides were imaged using ZEISS LSM 700 laser scanning confocal microscope as described previously (45).

For IHC, mice were euthanized 3 days after CAR T-cell injection and were perfused with PBS followed by 4% PFA. Whole brains were dissected and incubated in 4% PFA for 3 days, followed by 70% ethanol for 3 days before being embedded in paraffin. Transverse sections (10 μm thick) were cut and stained with hematoxylin and eosin or F4/80 (Abcam). Slides were digitized at 40× magnification using a NanoZoomer 2.0-HT digital slide scanner (Hamamatsu). The immunofluorescence of brain sections was performed on formalin-fixed, paraffin-embedded tissues as described previously (45). Myeloid cells in K-Luc tumors were evaluated using CD163 (Thermo Fisher Scientific), CD68, and CD206 (Abcam). Images were acquired by ZEISS LSM 700 laser scanning confocal microscope.

Luminex Cytokine Analysis

To assess CAR T-cell cytokine profile, mIL13Rα2-CAR$^+$ T cells and tumor cells (GL261-Luc-mIL13Rα2 or K-Luc-mIL13Rα2) were incubated at 1:1 ratio for 1 day without exogenous cytokines. The cell-free supernatant was collected and assayed using the ProcartaPlex Mouse Th1/Th2 Cytokine Panel 11plex (Thermo Fisher Scientific) according to the manufacturer's instructions and acquired on the Bio-Plex 3-D Suspension Array System (Bio-Rad Laboratories).

Quantitative PCR

All primers used for qPCR analysis are listed in Supplementary Table S2. RNA was isolated from myelin-removed brain tissue (either bulk tissue or flow sorted cells) using the RNeasy Mini Kit (Qiagen). cDNA was reverse-transcribed using the SuperScript VILO Mastermix (Life Technologies) according to the manufacturer's instructions. qPCR reactions were performed as described previously (42).

NanoString Gene Expression Analysis

RNA was purified from flow-sorted CD3$^+$ or CD11b$^+$ cells using the RNEasyPlus Micro Kit, following the manufacturer's instructions (Qiagen). RNA samples were subsequently quantified and qualified using Nanodrop 1000 Spectrophotometer (Thermo Fisher Scientific) and Bioanalyser Tape station (Agilent) assays. The subsequent NanoString analysis was performed at concentrations of 35 ng/well and 25 ng/well, respectively, for CD3$^+$ cells and CD11b$^+$ cells.

Samples were analyzed on the basis of the nCounter mouse Pan-Cancer Immune profiling gene expression panel (NanoString Technologies): Hybridation reaction was performed for 18 hours at 65°C. Fully automated nCounter FLEX analysis system; composed of an automated nCounter Prep station and the nCounter Digital Analyzer optical scanner (NanoString Technologies) was used. Normalization was performed by using the geometric mean of the positive control counts as well as normalization genes present in the CodeSet Content: samples with normalization factors outside of the 0.3–3.0 range were excluded, samples with reference factors outside the 0.10–10.0 range were excluded as well. Gene expression analysis was performed using the nSolver v3.0 and Advanced analysis module softwares (NanoString Technologies).

scRNA-seq

Seven days after K-Luc-mIL13Rα2 engraftment, CAR T cells were injected or not into the tumor as described above. Brains from CAR T-cell treated or untreated mice (n = 3 per group) were harvested and pooled three days after CAR T-cell injection, manually minced, and myelin removed before flow sorting on the BD AriaSORP (BD Biosciences) for live (DAPI$^-$) CD45$^+$ (BD Biosciences) cells. Single-cell suspensions were processed using the Chromium Single Cell 3′ v3 Reagent Kit (10× Genomics) and loaded onto a Chromium Single Cell Chip (10× Genomics) according to the manufacturer's instructions. Raw sequencing data from each of two experiments were aligned back to mouse genome (mm10), respectively, using cellranger count command to produce expression data at a single-cell resolution according to 10× Genomics (https://support.10xgenomics.com/single-cell-gene expression/software/pipelines/latest/using/count). R package Seurat (46) was used for gene and cell filtration, normalization, principal component analysis, variable gene finding, clustering analysis, and Uniform Manifold Approximation and Projection (UMAP) dimension reduction. Briefly, matrix containing gene-by-cell expression data was imported to create a Seurat object individually for CAR T cell–untreated and CAR T cell–treated samples. Cells with <200 detectable genes and a percentage of mitochondrial genes >10% were further removed. Data were then merged and log-normalized for subsequent analysis. Principal component analysis (PCA) was performed for dimension reduction, and the first 20 principal components were used for clustering analysis with a resolution of 0.6. Clusters were visualized with UMAP embedding. In addition to the use of Immunologic Genome Project (ImmGen; refs. 47, 48), to facilitate cell-type identification, the expression level of the following markers was

Published OnlineFirst April 9, 2021; DOI: 10.1158/2159-8290.CD-20-1661

plotted using VlnPlot. They were *Itagm*, *Cd3e*, *Cd19*, *Cd79a*, *Nkh7*, *Cd68*, and *Cd8a*. Upon the identification of lymphoid and myeloid parental clusters on each of them, we followed the above-mentioned strategy for subclustering to produce daughter clusters. In concert with ImmGen, key markers for distinguishing myeloid daughter clusters were *Itgam*, *Cd68*, *S100a9*, *Itgax*, *Tmem119*, and *P2ry12*, while for lymphoid *Cd3e*, *Cd4*, *Cd8a*, *Cd79a*, and *Ncr1*. To further visualize the average expression of a module of genes, *Cd74*, *H2-Aa*, *H2-Ab1*, *H2-Eb1*, and *Marcks*, across population in myeloid daughter clusters, AddModuleScore function was employed to generate a feature that could be rendered using FeaturePlot.

Gene Set Enrichment Analysis

Differentially expressed (DE) genes between untreated and CAR T cell–treated cells in each myeloid and lymphoid parental and daughter cluster were detected with function FindAllMarkers. The analysis on Gene Ontology (GO), Kyoto Encyclopedia of Genes and Genomes pathway, and Immunologic Signatures collection (ImmuneSigDB; ref. 49) was performed with the full list of DE genes of each cluster using GSEA function implemented in clusterProfiler package (50), then plotted with ggplot2 (H. Wickham. ggplot2: Elegant Graphics for Data Analysis. Springer-Verlag NY, 2016).

Statistical Analysis

Statistical significance was determined using Student *t* test (two groups) or one-way ANOVA with a Bonferroni (three or more groups). Survival was plotted using a Kaplan–Meier survival curve and statistical significance was determined by the log-rank (Mantel–Cox) test. All analyses were carried out using GraphPad Prism software (v5). *, $P < 0.05$; **, $P < 0.01$; ***, $P < 0.001$; ****, $P < 0.0001$.

Genomic Data Reporting and Sharing

scRNA-seq data sets have been deposited to the Gene Expression Omnibus (GSE168115) and will be accessible to the public at the time of publication.

Authors' Disclosures

D. Wang reports grants from NCI during the conduct of the study. N. Larmonier reports grants from Ligue Nationale Contre le Cancer and grants from SIRIC-BRIO during the conduct of the study. A. Ribas reports personal fees from Amgen, Chugai, Genentech, Merck, Novartis, Roche, Sanofi, and Vedanta; personal fees from Advaxis, Apricity, Arcus, Compugen, CytomX, Five Prime, Highlight, ImaginAb, Isoplexis, Kite-Gilead, Lutris, Merus, PACT, RAPT, Rgenix and Tango Therapeutics; and grants from Agilent and Bristol-Myers Squibb outside the submitted work. B. Badie reports grants from NIH and other support from Mustang Therapeutics during the conduct of the study and other support from Mustang Therapeutics outside the submitted work; in addition, B. Badie has a patent for CAR T-cell delivery pending and with royalties paid from Mustang Therapeutics. C.E. Brown reports other support from Mustang Bio, grants from NCI, and grants from CIRM during the conduct of the study; personal fees and other support from Chimeric Therapeutics and personal fees and other support from Mustang Bio outside the submitted work; in addition, C.E. Brown has a patent pending. No disclosures were reported by the other authors.

Authors' Contributions

D. Alizadeh: Conceptualization, data curation, formal analysis, supervision, methodology, writing–original draft, writing–review and editing. **R.A. Wong:** Data curation, formal analysis, methodology, writing–review and editing. **S. Gholamin:** Data curation, methodology, writing–review and editing. **M. Maker:** Data curation, methodology, writing–review and editing. **M. Aftabizadeh:** Data curation, methodology. **X. Yang:** Methodology. **J.R. Pecoraro:** Methodology. **J.D. Jeppson:** Methodology, writing–review and editing. **D. Wang:** Methodology, writing–review and editing. **B. Aguilar:** Resources, methodology. **R. Starr:** Resources, data curation, methodology. **C.B. Larmonier:** Data curation, methodology, writing–review and editing. **N. Larmonier:** Software, formal analysis, writing–review and editing. **M. Chen:** Data curation, software, formal analysis. **X. Wu:** Data curation, software, writing–review and editing. **A. Ribas:** Writing–review and editing. **B. Badie:** Writing–review and editing. **S.J. Forman:** Conceptualization, funding acquisition, writing–original draft, writing–review and editing. **C.E. Brown:** Conceptualization, data curation, funding acquisition, writing–original draft, writing–review and editing.

Acknowledgments

This work was supported in part by Mustang Bio., Inc., R01-CA236500 (to D. Alizadeh, R.A. Wong, C.E. Brown), CA234923 (to D. Wang), California Institute for Regenerative Medicine CLIN2-10248 (to D. Alizadeh, R.A. Wong, C.E. Brown), Ben and Catherine Ivy Foundation (to D. Alizadeh, R.A. Wong, M. Maker, C.E. Brown), Ligue Nationale contre le Cancer and SIRIC-BRIO (to N. Larmonier), and Cancer Center Support Grant P30 CA33572. S. Gholamin is a Parker Institute scholar. Patents associated with IL13Rα2-CAR T have been licensed by Mustang Bio., Inc., for which S.J. Forman and C.E. Brown receive royalty payments. The authors would like to thank Leo D. Wang MD, PhD, for critical paper review and feedback, and the technical assistance of Jinhui Wang, Ryan Urak, Supraja Saravanakumar, Charles Warden, and Aniee Sarkissian.

Received November 16, 2020; revised February 24, 2021; accepted April 5, 2021; published first April 9, 2021.

REFERENCES

1. McGranahan T, Therkelsen KE, Ahmad S, Nagpal S. Current state of immunotherapy for treatment of glioblastoma. Curr Treat Options Oncol 2019;20:24.
2. Alexander BM, Cloughesy TF. Adult glioblastoma. J Clin Oncol 2017;35:2402–9.
3. Medikonda R, Dunn G, Rahman M, Fecci P, Lim M. A review of glioblastoma immunotherapy. J Neurooncol 2021;151:41–53.
4. Akhavan D, Alizadeh D, Wang D, Weist MR, Shepphird JK, Brown CE. CAR T cells for brain tumors: lessons learned and road ahead. Immunol Rev 2019;290:60–84.
5. Hegde M, Corder A, Chow KK, Mukherjee M, Ashoori A, Kew Y, et al. Combinational targeting offsets antigen escape and enhances effector functions of adoptively transferred T cells in glioblastoma. Mol Ther 2013;21:2087–101.
6. Brown CE, Aguilar B, Starr R, Yang X, Chang WC, Weng L, et al. Optimization of IL13Ralpha2-targeted chimeric antigen receptor T cells for improved anti-tumor efficacy against glioblastoma. Mol Ther 2018;26:31–44.
7. Wang D, Starr R, Chang WC, Aguilar B, Alizadeh D, Wright SL, et al. Chlorotoxin-directed CAR T cells for specific and effective targeting of glioblastoma. Sci Transl Med 2020;12:eaaw2672.
8. Hu B, Ren J, Luo Y, Keith B, Young RM, Scholler J, et al. Augmentation of antitumor immunity by human and mouse CAR T cells secreting IL-18. Cell Rep 2017;20:3025–33.
9. Chmielewski M, Kopecky C, Hombach AA, Abken H. IL-12 release by engineered T cells expressing chimeric antigen receptors can effectively Muster an antigen-independent macrophage response on tumor cells that have shut down tumor antigen expression. Cancer Res 2011;71:5697–706.
10. Krenciute G, Prinzing BL, Yi Z, Wu MF, Liu H, Dotti G, et al. Transgenic expression of IL15 improves antiglioma activity of IL13Ralpha2-CAR T cells but results in antigen loss variants. Cancer Immunol Res 2017;5:571–81.
11. Kershaw MH, Wang G, Westwood JA, Pachynski RK, Tiffany HL, Marincola FM, et al. Redirecting migration of T cells to chemokine

Published OnlineFirst April 9, 2021; DOI: 10.1158/2159-8290.CD-20-1661

secreted from tumors by genetic modification with CXCR2. Hum Gene Ther 2002;13:1971–80.
12. Pituch KC, Miska J, Krenciute G, Panek WK, Li G, Rodriguez-Cruz T, et al. Adoptive transfer of IL13Ralpha2-specific chimeric antigen receptor T cells creates a pro-inflammatory environment in glioblastoma. Mol Ther 2018;26:986–95.
13. Avanzi MP, Yeku O, Li X, Wijewarnasuriya DP, van Leeuwen DG, Cheung K, et al. Engineered tumor-targeted T cells mediate enhanced anti-tumor efficacy both directly and through activation of the endogenous immune system. Cell Rep 2018;23:2130–41.
14. Duluc D, Corvaisier M, Blanchard S, Catala L, Descamps P, Gamelin E, et al. Interferon-gamma reverses the immunosuppressive and pro-tumoral properties and prevents the generation of human tumor-associated macrophages. Int J Cancer 2009;125:367–73.
15. Rock RB, Hu S, Deshpande A, Munir S, May BJ, Baker CA, et al. Transcriptional response of human microglial cells to interferon-gamma. Genes Immun 2005;6:712–9.
16. Castro F, Cardoso AP, Goncalves RM, Serre K, Oliveira MJ. Interferon-gamma at the crossroads of tumor immune surveillance or evasion. Front Immunol 2018;9:847.
17. Bhat P, Leggatt G, Waterhouse N, Frazer IH. Interferon-gamma derived from cytotoxic lymphocytes directly enhances their motility and cytotoxicity. Cell Death Dis 2017;8:e2836.
18. Dunn GP, Koebel CM, Schreiber RD. Interferons, immunity and cancer immunoediting. Nat Rev Immunol 2006;6:836–48.
19. Curtsinger JM, Mescher MF. Inflammatory cytokines as a third signal for T cell activation. Curr Opin Immunol 2010;22:333–40.
20. Brown CE, Alizadeh D, Starr R, Weng L, Wagner JR, Naranjo A, et al. Regression of glioblastoma after chimeric antigen receptor T-cell therapy. N Engl J Med 2016;375:2561–9.
21. Hegde M, Joseph SK, Pashankar F, DeRenzo C, Sanber K, Navai S, et al. Tumor response and endogenous immune reactivity after administration of HER2 CAR T cells in a child with metastatic rhabdomyosarcoma. Nat Commun 2020;11:3549.
22. O'Rourke DM, Nasrallah MP, Desai A, Melenhorst JJ, Mansfield K, Morrissette JJD, et al. A single dose of peripherally infused EGFRvIII-directed CAR T cells mediates antigen loss and induces adaptive resistance in patients with recurrent glioblastoma. Sci Transl Med 2017;9:eaaa0984.
23. Ahmed N, Brawley V, Hegde M, Bielamowicz K, Kalra M, Landi D, et al. HER2-specific chimeric antigen receptor-modified virus-specific T cells for progressive glioblastoma: a phase 1 dose-escalation trial. JAMA Oncol 2017;3:1094–101.
24. Goff SL, Morgan RA, Yang JC, Sherry RM, Robbins PF, Restifo NP, et al. Pilot trial of adoptive transfer of chimeric antigen receptor-transduced T cells targeting EGFRvIII in patients with glioblastoma. J Immunother 2019;42:126–35.
25. Brown CE, Warden CD, Starr R, Deng X, Badie B, Yuan YC, et al. Glioma IL13Ralpha2 is associated with mesenchymal signature gene expression and poor patient prognosis. PLoS One 2013;8:e77769.
26. Reilly KM, Loisel DA, Bronson RT, McLaughlin ME, Jacks T. Nf1;Trp53 mutant mice develop glioblastoma with evidence of strain-specific effects. Nat Genet 2000;26:109–13.
27. Flores CT, Wildes TJ, Drake JA, Moore GL, Dean BD, Abraham RS, et al. Lin(-)CCR2(+) hematopoietic stem and progenitor cells overcome resistance to PD-1 blockade. Nat Commun 2018;9:4313.
28. Ausman JI, Shapiro WR, Rall DP. Studies on the chemotherapy of experimental brain tumors: development of an experimental model. Cancer Res 1970;30:2394–400.
29. Reardon DA, Gokhale PC, Klein SR, Ligon KL, Rodig SJ, Ramkissoon SH, et al. Glioblastoma eradication following immune checkpoint blockade in an orthotopic, immunocompetent model. Cancer Immunol Res 2016;4:124–35.
30. Gutmann DH, Kettenmann H. Microglia/brain macrophages as central drivers of brain tumor pathobiology. Neuron 2019;104:442–9.
31. Quail DF, Joyce JA. The microenvironmental landscape of brain tumors. Cancer Cell 2017;31:326–41.
32. Schulz EG, Mariani L, Radbruch A, Hofer T. Sequential polarization and imprinting of type 1 T helper lymphocytes by interferon-gamma and interleukin-12. Immunity 2009;30:673–83.
33. Cloughesy TF, Mochizuki AY, Orpilla JR, Hugo W, Lee AH, Davidson TB, et al. Neoadjuvant anti-PD-1 immunotherapy promotes a survival benefit with intratumoral and systemic immune responses in recurrent glioblastoma. Nat Med 2019;25:477–86.
34. Gieryng A, Pszczolkowska D, Walentynowicz KA, Rajan WD, Kaminska B. Immune microenvironment of gliomas. Lab Invest 2017;97:498–518.
35. Jansen CS, Prokhnevska N, Master VA, Sanda MG, Carlisle JW, Bilen MA, et al. An intra-tumoral niche maintains and differentiates stem-like CD8 T cells. Nature 2019;576:465–70.
36. Corrales L, McWhirter SM, Dubensky TW Jr, Gajewski TF. The host STING pathway at the interface of cancer and immunity. J Clin Invest 2016;126:2404–11.
37. Yao Y, Jeyanathan M, Haddadi S, Barra NG, Vaseghi-Shanjani M, Damjanovic D, et al. Induction of autonomous memory alveolar macrophages requires T cell help and is critical to trained immunity. Cell 2018;175:1634–50.
38. Grasso CS, Tsoi J, Onyshchenko M, Abril-Rodriguez G, Ross-Macdonald P, Wind-Rotolo M, et al. Conserved interferon-gamma signaling drives clinical response to immune checkpoint blockade therapy in melanoma. Cancer Cell 2021;39:122.
39. Dunn GP, Old LJ, Schreiber RD. The three Es of cancer immunoediting. Annu Rev Immunol 2004;22:329–60.
40. Kuhn NF, Purdon TJ, van Leeuwen DG, Lopez AV, Curran KJ, Daniyan AF, et al. CD40 ligand-modified chimeric antigen receptor T cells enhance antitumor function by eliciting an endogenous antitumor response. Cancer Cell 2019;35:473–88.
41. Klampatsa A, Leibowitz MS, Sun J, Liousia M, Arguiri E, Albelda SM. Analysis and augmentation of the immunologic bystander effects of CAR T cell therapy in a syngeneic mouse cancer model. Mol Ther Oncolytics 2020;18:360–71.
42. Wang D, Aguilar B, Starr R, Alizadeh D, Brito A, Sarkissian A, et al. Glioblastoma-targeted CD4+ CAR T cells mediate superior antitumor activity. JCI insight 2018;3:e99048.
43. Brown CE, Starr R, Martinez C, Aguilar B, D'Apuzzo M, Todorov I, et al. Recognition and killing of brain tumor stem-like initiating cells by CD8+ cytolytic T cells. Cancer Res 2009;69:8886–93.
44. Dudley ME, Rosenberg SA. Adoptive-cell-transfer therapy for the treatment of patients with cancer. Nat Rev Cancer 2003;3:666–75.
45. Zhang C, Yue C, Herrmann A, Song J, Egelston C, Wang T, et al. STAT3 activation-induced fatty acid oxidation in CD8(+) T effector cells is critical for obesity-promoted breast tumor growth. Cell Metab 2020;31:148–61.
46. Stuart T, Butler A, Hoffman P, Hafemeister C, Papalexi E, Mauck WM III, et al. Comprehensive integration of single-cell data. Cell 2019;177:1888–902.
47. Heng TS, Painter MW, Immunological Genome Project Consortium. The Immunological Genome Project: networks of gene expression in immune cells. Nat Immunol 2008;9:1091–4.
48. Aran D, Looney AP, Liu L, Wu E, Fong V, Hsu A, et al. Reference-based analysis of lung single-cell sequencing reveals a transitional profibrotic macrophage. Nat Immunol 2019;20:163–72.
49. Godec J, Tan Y, Liberzon A, Tamayo P, Bhattacharya S, Butte AJ, et al. Compendium of immune signatures identifies conserved and species-specific biology in response to inflammation. Immunity 2016;44:194–206.
50. Yu G, Wang LG, Han Y, He QY. clusterProfiler: an R package for comparing biological themes among gene clusters. OMICS 2012;16:284–7.

Published OnlineFirst April 9, 2021; DOI: 10.1158/2159-8290.CD-20-1661

AACR American Association for Cancer Research

CANCER DISCOVERY

IFNγ Is Critical for CAR T Cell –Mediated Myeloid Activation and Induction of Endogenous Immunity

Darya Alizadeh, Robyn A. Wong, Sharareh Gholamin, et al.

Cancer Discov 2021;11:2248-2265. Published OnlineFirst April 9, 2021.